Glacitectonic evidence of ice sheet interaction and retreat across the western part of Dogger Bank (North Sea) during the Last Glaciation

Emrys Phillips[1]*, Kirstin Johnson[1], Rachael Ellen[1], Gayle Plenderleith[1], Dayton Dove[1], Gareth Carter[1], Nicola Dakin[1] and Carol Cotterill[1,2]

1. British Geological Survey, The Lyell Centre, Research Avenue South, Riccarton, Edinburgh, EH14 4AS, Scotland, UK

2. 212B Lamont-Doherty Earth Observatory, 61 Rte 9W, Palisades, NY 10964, USA

*corresponding author: erp@bgs.ac.uk

Abstract

High-resolution 2D seismic data from the western side of Dogger Bank (North Sea) has revealed that the glacigenic sediments of the Dogger Bank Formation record a complex history of sedimentation and penecontemporaneous, large-scale, ice-marginal to proglacial glacitectonism. The resulting complex assemblage of glacial landforms and sediments record the interplay between two separate ice masses revealing that Weichselian ice sheet dynamics across Dogger Bank were far more complex than previously thought, involving the North Sea lobe of the British and Irish Ice Sheet, advancing from the west, interacting with the Dogger Bank lobe which expanded from the north. The active northward retreat of the Dogger Bank lobe resulted in the development of a complex assemblage of arcuate thrust-block moraines (≤15km wide, >30km long) composed of highly folded and thrust sediments, separated by sedimentary basins and meltwater channels filled by outwash. The impact of the North Sea lobe was restricted to the western margin of Dogger Bank and led to deep-seated (100-150m thick) glacitectonism in response to ice-push from the west. During the earlier expansion of the North Sea lobe, this thrust and fold complex initially occupied a frontal marginal position changing to a more lateral ice-marginal position as the ice sheet continued to expand to the south. The complex structural relationships between the two glacitectonic complexes indicates that these ice masses interacted along the western side of Dogger Bank, with the inundation of this area by ice probably occurring during the last glaciation when the ice sheets attained their maximum extents.

Keywords

Glacitectonics; ice-lobe interaction; Dogger Bank; North Sea; high-resolution seismic data; Late Devensian glaciation

1. Introduction

The recent geological history of the North Sea basin (*c*. 500 km wide, 50-400 m deep) which separates the UK from Scandinavia and northern mainland Europe (Fig. 1) was dominated by the deposition of a locally thick (≥800 m) sequence of Quaternary sediments (Cameron et al., 1987; Caston, 1977, 1979; Holmes, 1977; Gatliff et al., 1994; Huuse, 2002; Anell et al., 2010, 2012; Głędowski et al., 2012; Fyfe et al., 2013; Ottesen et al., 2014; Lamb et al., 2017). This sequence contains evidence of at least three major glaciations, the Elsterian (oldest, Marine Isotope Stage (MIS) 12), Saalian (MIS 10-6), and the Weichselian (Europe) or Devensian (UK) (youngest, MIS 2), separated by warmer interglacial periods (Eisma et al., 1979; Jansen et al., 1979; Caston 1979; Balson and Cameron, 1985; Sejrup et al., 1987, 1995, 2000, 2003; Cameron et al., 1987, 1992; Ehlers, 1990; Beets et al., 2005; Lonergan et al., 2006; Graham et al., 2007, 2011; Kristensen et al., 2007; Bradwell et al., 2008; Stewart and Lonergan, 2011; Stoker et al., 2011; Bose et al., 2012; Stewart et al., 2013; Ottesen et al., 2014, 2018; Phillips et al., 2017). During these glacial episodes several major ice sheets advanced into the North Sea basin from the surrounding land masses. Consequently, the Quaternary of the North Sea is critical to our understanding of the evolution of the major European ice masses, in particular the British and Irish (BIIS) and Fennoscandian (FIS) ice sheets and reveals that these palaeo-ice masses periodically extended to the margins of the continental shelf (Graham et al., 2007, 2010, 2011; Bradwell et al., 2008; Dunlop et al., 2010; Howe et al., 2012; Lee et al., 2012).

Several published models argue that during the last glaciation the BIIS (Devensian) and FIS (Weichselian) converged within the central part of the North Sea basin (e.g. Boulton and Hagdorn, 2006; Carr et al., 2006; Graham et al., 2007, 2011; Bradwell et al., 2008; Sejrup et al., 2009, 2016; Hughes et al., 2016). However, the maximum extents of these ice sheets are as yet poorly constrained (see Fig. 1) (*e.g*. Jansen et al., 1979; Catt, 1991; Clark et al., 2004; Hubbard et al., 2009; Brooks et al., 2009; Sejrup et al., 2009, 2016). This uncertainty partly resulted from the fact that, until recently, very little was known about the Quaternary sequence underlying Dogger Bank; an isolated, approximately NE-SW-trending bathymetric high (100 km wide, 250 km long, water depths 18-63 m Lowest Astronomical Tide (LAT)) located within the southern central North Sea in an area likely to occur in the southern confluence zone between the BIIS and FIS (Fig. 1). The sedimentary sequence in this area was originally thought to comprise a tabular unit of well-bedded sediments, the Dogger Bank Formation (DBF), laid down in a proglacial setting or ice-dammed lake trapped along the confluence

between the BIIS and FIS (Cameron et al., 1992; also see Valentin, 1955; Veenstra, 1965). Although this interpretation relied heavily on the extrapolation of seismic stratigraphies from adjacent areas, the existence of a regional scale glacial lake on Dogger Bank has been widely adopted in the literature (see Clarke et al., 2012; Hijma et al., 2012; Cohen et al., 2014; Sejrup et al., 2016; Hjelstuen et al., 2017; Roberts et al., 2018). However, several recently published studies have revealed the complexity of the sedimentary architecture (Cotterill et al., 2017a; Emery et al., 2019) and glacitectonic deformation (Cotterill et al., 2017b; Phillips et al., 2018; Roberts et al., 2018) recorded by the DBF, confirming earlier hypotheses that Dogger Bank comprises a series of moraines buried beneath younger sediments (Belt, 1874; Stride, 1959; Veenstra, 1965; van der Meer and Laban, 1990; Laban, 1995).

Using high-resolution 2D seismic data acquired during the early stages of the site survey for a major offshore windfarm located on Dogger Bank, Cotterill et al. (2017a) demonstrated that the underlying Quaternary sequence records the complex interplay between climatic variation, sea level changes (rise and fall) and ice sheet movement. Furthermore, the data revealed that ice sheet dynamics during the last glaciation (Devensian/Weichselian) were far more complex than previously thought with Dogger Bank having been inundated by ice on more than one occasion. Phillips et al. (2018) concluded that the construction of an extensive landsystem of thrust-block moraines and intervening sedimentary basins in the southwest part of Dogger Bank (buried beneath younger Holocene sediments) occurred during the active north/northwest retreat of a Devensian ice sheet. Comparable glaciotectonic complexes comprising folded and thrusted glacigenic sediments have been described elsewhere within the North Sea basin and adjacent areas where they are associated with glaciations of different ages (*e.g*. Huuse et al., 2001; Andersen et al., 2005; Phillips et al., 2008; Burke et al., 2009; Bakker and van der Meer, 2015; Vaughan-Hirsch and Phillips, 2017; Lee et al., 2013, 2017; Pedersen and Boldreel, 2017). To the east of the Dogger Bank glacitectonic landsystem, Emery et al. (2019) provided sedimentological and seismostratigraphical evidence for the presence of a large (*c*. 750 km^2) proglacial lake which was progressively infilled by an undeformed sequence of glacial outwash and lacustrine sediments (also see Cotterill et al., 2017a). This lake is thought to have been dammed by a large thrust-block moraine which Emery et al. (2019) interpreted as a 'terminal moraine' that marked the maximum extent of glacier ice on Dogger Bank. In a separate study, Roberts et al. (2018) suggest that the glacilacustrine sediments underlying part of Dogger Bank were deposited between 31.6 and 25.8 ka, and that the northwards retreat of the Late Devensian ice sheet from Dogger Bank had been completed by 23.1 ka. Although these studies have led to an advance in our understanding of the Quaternary evolution of this sector of the North Sea, a large part of the central and eastern parts of Dogger Bank have yet to be investigated. Consequently, significant parts of the Late Devensian glacial history (equivalent to the Late Weichselian glaciation in Europe) of the region remain uncertain.

This paper aims to begin to address this knowledge gap by investigating the Late Devensian (MIS 2) glacial history of the western margin of Dogger Bank (Fig. 1), building upon the previously published studies of Cotterill et al. (2107) and Phillips et al. (2018). High-resolution 2D sub-bottom seismic profiles are used to construct detailed cross-sections through the DBF, revealing a complex history of sedimentation and penecontemporaneous large-scale glacitectonism. This complexity is used to suggest that the glacigenic sequence records the interplay between two discrete ice masses. The first advanced from the north/northwest and was responsible for the thin-skinned (*c*. 40-50 m thick) thrusting and folding described by Phillips et al. (2018) during the active retreat of this highly dynamic ice mass towards the north. In contrast, the impact of the second ice mass was restricted to the western edge of Dogger Bank and led to the formation of a much thicker (*c*. 100-150 m thick) glacitectonised sequence associated with ice advancing from the west. Detailed cross-sections through the boundary zone between the two ice masses are used to investigate how they interacted during the early stages of ice sheet retreat from this part of Dogger Bank.

2. Methods

The high-resolution 2D sub-bottom seismic profiles (Sparker - inline spacing, 100 m; crossline, 500-1000 m) used in this study were acquired as part of a detailed site investigation for the Dogger Bank windfarm (125-290 km to the northeast of the Yorkshire coast; Fig. 1) by the Forewind consortium (Equinor, SSE, Statkraft, RWE and Npower Renewables). Initial analysis of the data identified several laterally extensive seismic reflections which can be traced across Dogger Bank and are key to understanding the evolution of the area (Cotterill et al., 2017a, b; Phillips et al., 2018). The reflection forming the boundary between the lower and upper units of the DBF was gridded and the resultant 'horizon map' (Fig. 2a) interpreted in terms of an ice-marginal to proglacial glacitectonic landsystem (Fig. 2b; after Phillips et al., 2018), buried beneath younger sediments. The red colours on Fig. 2a represent areas where this boundary occurs closer to the seabed (shallower depth), representing the crests of the topographically higher moraines (compare Fig. 2a and b). Whereas the green colours (Fig. 2a) highlight areas where the boundary is at a deeper level, corresponding to topographically lower sedimentary basins developed between the moraines. A total of 34 2D seismic profiles were analysed from three key areas (Areas A, B and C, Fig. 2) to gain a greater understanding of the structural and sedimentary architecture of the DBF underlying the western part of Dogger Bank. The resulting geological cross-sections are shown in Figs. 3, 4 and 5, and are available as high-resolution digital (jpeg) versions as both supplementary publications and from the first author on request.

The individual seismic profiles were exported from IHS Kingdom® as high-resolution digital image files (jpegs) and imported into a commercial computer graphics package (CorelDraw ™) to carry out the detailed analysis. Different line styles were used for particular geological structures (bedding, fold axes, thrusts and faults) and coloured polygons to represent the individual seismo/tectonostratigraphic units, as well as the constituent sedimentary subunits (identified on the basis of differences in their acoustic properties) within the relatively undeformed upper part of the DBF. The colours used do not infer any direct correlation as seismostratigraphic units, but rather serve to highlight the geometry of the individual sediment packages. An approximate depth conversion used to aid correlation of the structural/sedimentological features and thicknesses of the units were obtained using the following velocities (based on previous velocities gained from glacial sediments in the North Sea by RPS Energy): Water Column – 1550 m/s; Holocene sediments – 1600 m/s; upper Dogger Bank – 1680 m/s; and lower Dogger Bank – 1750 m/s.

3. Stratigraphy of the Quaternary sequence underlying Dogger Bank

The Quaternary sequence in the Dogger Bank area (≤800 m thick) was divided by Stoker et al. (2011) into three major groups: *(i)* Southern North Sea Deltaic Group (oldest) ranging in age from Early Pleistocene to early Middle Pleistocene; *(ii*) Dunwich Group comprising a deltaic sequence of early Middle Pleistocene age; and *(iii)* the late Middle Pleistocene to Holocene age Californian Glacigenic Group (youngest). Cotterill et al. (2017a) divided the upper part of Californian Glacigenic Group sequence underlying the western part of Dogger Bank into three main units: *(i)* the interglacial Eem Formation (oldest, Eemian/Ipswichian, MIS 5e) comprising silty to fine-grained marine (shelly) sands with interbeds of hard clay and silty fine sand; *(ii)* the Dogger Bank Formation (≤50-60 m thick) composed of generally stiff to very stiff silts and clays containing multiple sand layers; and *(iii)* an overlying thin (<1m thick) sequence of fine- to medium-grained Holocene sands (youngest) which are locally being reworked by contemporary marine processes.

Cotterill et al. (2017a, b) and Phillips et al. (2018) further subdivided the DBF into three informal tectonostratigraphic subunits (basal, lower and upper Dogger Bank; Table 1), the boundaries between these units being marked by laterally extensive bands of strong/bright reflectors which have been interpreted as desiccation surfaces (palaeo-land surfaces) which may have formed as a result of periglacial weathering and alteration (Norwegian Geotechnical Institute, unpublished data). Phillips et al. (2018) demonstrated that the highly deformed (purple colours, Figs. 3, 4 and 5) lower part of the DBF (5-40 m thick) is folded and thrust into a series of large, ridge-like thrust-block moraines (red colours, Fig. 2a). These glacitectonised sediments are overlain by a largely undeformed, often

acoustically well-layered (bedded) sequence of upper Dogger Bank sediments (≤5-40 m thick) (green colours, Figs. 3, 4 and 5) which infill the sedimentary basins located between the moraine ridges (Fig. 2b). Although widely described as being composed of clay and silt, logging of cores obtained during the ongoing windfarm site survey indicates that the DBF also contains sands (locally micaceous) and rare gravels which form a thin, laterally discontinuous layer along the base of the upper DBF. The presence of organic material within these sands provides clear evidence that the DBF was deposited in a terrestrial environment with land surfaces periodically undergoing prolonged periods of periglacial weathering (Cotterill et al., 2017a).

4. Structural and sedimentary architecture of Dogger Bank

For ease of description the subsurface geology of the western part of Dogger Bank has been divided into three areas (Fig. 2): *(i)* ***Area A***, to the south, in which the structural and sedimentary architecture of the DBF records the active north/northwest retreat of the ice sheet (Phillips et al., 2018); (ii) ***Area B*** which includes a northward extension of the thrust-block moraine complex recognised in Area A, but also a more deep-seated glacitectonised sequence along its western margin (FTC on Fig. 3); and *(iii)* ***Area C*** which occurs between the other two areas and characterised by a much simpler subsurface structure. The subsurface geology of Area A (Fig. 3) has previously been described in detail by Phillips et al. (2018) and is only summarised here, with areas B (Fig. 4) and C (Fig. 5) forming the focus of this study.

4.1. Area A: evidence of glacitectonic deformation and associated sedimentation

Cross-sections through this area (seismic profiles 1–4, Fig. 2a) reveal that the relative intensity and complexity of deformation, as well as the thickness of the deformed lower part of the DBF, increase rapidly towards the northeast (Fig. 3), coinciding with the core of a large (15-20 km wide), structurally complex thrust-block moraine (TBM1, Fig. 2b). The tops of the large moraine ridges (originally over 40-50 m high) have been eroded/truncated during the deposition of the upper DBF and/or the later Holocene sedimentary sequence (Fig. 3). Deformation of the lower DBF is dominated by NE-dipping thrusts and associated SW-verging folds (Fig. 3) which developed in response to ice-push directed towards the S/SW. Poorly resolved areas on the seismic data which appear acoustically blank with very few, if any, recognisable reflectors and are interpreted as intensely deformed parts of the sequence. However it is also possible that these acoustically blank areas may, at least in part, represent mass flows deposited at the ice margin. Elsewhere the reflectors are dissected and offset by thrusts propagating upwards from a prominent, subhorizontal to gently N-dipping décollement marking the base of the DBF. This basal décollement may also have affected the underlying Eem Formation leading to the incorporation of thrust-bound glacitectonic rafts of these older sediments

into the thrust-block moraines. Phillips et al. (2018) concluded that these arcuate glacitectonic landforms developed as the oscillating ice sheet repeatedly reoccupied essentially the same ice marginal position (see fig. 12 of Phillips et al., 2018). This not only resulted in the accretion of a relatively younger thrust and folded sediment onto the up-ice side of the evolving moraine complex, but also folding of earlier formed structures (polyphase deformation).

The upper DBF is typically undeformed with the variation in acoustic properties and changes in dip of the reflectors (bedding) enabling this sequence to be divided into several locally well-bedded, tabular to lenticular sedimentary packages separated by prominent erosion surfaces (Fig. 3) (Phillips et al., 2018). Inclined, SW-dipping reflectors are interpreted as foresets recording the southerly progradation of a series of outwash fans or aprons into the forefield of the retreating ice sheet. These fans were fed by meltwater channels incised into their upper surfaces (Fig. 3a to c) and represented the establishing of a more stable channelised meltwater drainage system. Localised folding and thrusting of the upper DBF is consistent with the deposition of at least the early part of this outwash sequence having accompanied glacitectonism (Phillips et al., 2018). The more tabular to sheet-like packages are considered to represent laterally more extensive outwash deposits laid down as the ice sheet retreated northward.

Elsewhere within Area A, the upper DBF infills several large (≤2-3 km wide), deeply incised (≤40-60 m deep) channels which locally cut through the lower DBF and into the underlying Eem Formation (fig. 4 of Phillips et al., 2018). These large channels are thought to reflect an increase in the volume of meltwater being liberated by the retreating ice, possibly forming due to the coalescing of several smaller channels. The complex nature of the sedimentary infills suggests that the large channels were active over a prolonged period, potentially forming a stable glaciofluvial network which drained meltwater from the forefield of the retreating ice sheet (Fig. 2b).

4.2. Area B: evidence of "shallow" glacitectonic thrusting and folding

The subsurface geology in Area B (seismic profiles 5–15, Fig. 2a) is characterised by a series of NW-SE-trending moraines (20-50 m high, ≤5-10 km across) composed of folded and thrust lower DBF (Figs. 4, 6 and 7). The individual thrust-block moraines (TBM) are composite landforms comprising a series of ridges buried beneath a thin cover sequence of undeformed upper DBF sediments and are considered to represent the lateral continuation of the suite of glacitectonic landforms identified in Area A (Fig. 2). Deformation of the lower DBF in Area B is dominated by W/SW-directed thrusting and symmetrical to asymmetrical SW-verging folding (wavelengths 50-200 m) (Figs. 4 and 6), consistent with ice-push towards the W/SW. The wedge-shaped to mound-like moraines exhibit a tapered southwest leading-edge, thickening rapidly northeast wards (from *c.* 5 m up to 40-50 m, within 3-4 km) accompanied by an increase in the relative intensity and complexity of deformation (Fig. 4a, I, k). Bands of moderate

to well-developed reflectors within this deformed sequence are offset by NE-dipping thrusts and SW-dipping high-angle (normal and reverse) faults (Fig. 6). The thrusts propagate upwards from a basal décollement located at, or close to, the boundary with the structurally underlying Eem Formation (*c*. 40-50 m below seabed). The internal structure of the moraines varies from landforms in which deformation is dominated by folding and moderately inclined thrusting (Fig. 4b), to those composed of laterally extensive subhorizontal thrust-bound, imbricate slabs of variably folded lower DBF which occur immediately to the southwest (down-ice) of prominent ramps (10-15 m high) within the décollement (Figs. 4e, f, g and 7), or a combination of these two structural styles (Fig. 4f, g). Variation in the geometry (Z, M and S) and vergence (NE to SW) of mesoscale folds within the lower DBF reveals the presence of large-scale anticlines and synclines with wavelengths up to 4 km. The similarity in the thin-skinned style of the deformation in both Areas A and B is consistent with this buried glacitectonic landsystem having formed in response to S/SW-directed ice-push during the active retreat of a lobate ice margin with the thrust-block moraines in Area B occupying a more lateral-marginal position.

The individual thrust-block moraines in Area B are separated by 2-5 km wide basins or narrower linear features (possible large 100-500 m wide channels) filled by a complex sequence of variably deformed upper DBF sediments which thin laterally onto the adjacent glacitectonic landforms (Figs. 4a, d, f, g, h, 7 and 7). The ice-marginal to proglacial basins can be traced laterally between the seismic profiles and typically become wider towards the S (Fig. 4). The variation in the acoustic properties of the upper DBF reveals that the basins are filled by a series of lenticular to laterally more extensive, tabular sediment packages separated by locally prominent erosion surfaces and incised by meltwater channels range from a few 10's m to several km across (Fig, 4b. f, g). Inclined reflectors within the lenticular sediment packages (Fig. 4h) are, once again, interpreted as foresets formed by prograding ice marginal fans/aprons. Desiccation surfaces within the upper DBF (marked by bands of bright reflectors) are thought to record significant breaks in deposition, possibly reflecting marked changes in the pattern of sedimentation within the forefield of the retreating ice sheet. The base of the upper DBF not only truncates deformation structures within the underlying glacitectonic landforms, but in the case of one of the larger basins, cuts downwards into the pre-DBF sediments of the California Glacigenic Group (Figs. 6 and 7). The complex sedimentary fill to this deep (50-70 m) linear basin (Fig. 4f, g, h) includes several incised channels which will have drained meltwater away from the retreating ice margin. The sediments filling the lower part of the basin thin onto the moraine located immediately to the south. However, on the northeast-side of the basin the upper DBF is deformed (folded) and truncated against the leading edge of the adjacent thrust-block moraine (Fig. 6).

4.3. Area B: evidence of deep-seated glacitectonic thrusting and folding

In contrast to the relatively shallow nature of the deformation dominating the shallow subsurface structure of areas A and B, glacitectonism along western margin of Area B (see Fig. 2) is characterised by a deep-seated (100-150m thick), large scale (≤20 km across), lenticular to wedge-shaped fold and thrust complex (pale blue colour, Fig. 4). In contrast to the gently to moderately sloping southwest-margin of this fold and thrust complex (FTC), its northeast-side is more steeply inclined and displays a complex relationship with the leading edge of the thrust-block moraines (TBM) immediately to the northeast (Figs. 8 and 9). Cross-sections shown in Fig. 4 indicate that the FTC becomes progressively wider and structurally more complex from north (Fig. 4a) to south (Fig. 4g), before apparently narrowing again close to the southern margin of Area B (Fig. 4k). The scale of the deformation indicates that glacitectonism not only affected the DBF, but must have also incorporated part of the underlying Californian Glacigenic Group succession (*e.g*. Eem and Egmond Ground formations). The top of the FTC is truncated against the base of a thin Holocene sequence and/or seabed indicating that it would have originally formed a prominent topographic feature within the glacial landscape.

Bright reflectors on the seismic profiles are disrupted by E/NE-directed thrusts and associated E/NE-verging folds (Figs. 4, 8 and 10) indicative of ice-push towards the east; in marked contrast to the SW-directed glacitectonic deformation identified elsewhere within Area B. The FTC can be subdivided into: an older, structurally lower domain in which the reflectors and thrusts dip at low to moderate angles towards the SW; and a structurally higher, relatively younger domain characterised by NE-verging asymmetrical, tight to open folds separated by over steepened thrusts (Figs. 4, 8 and 10). The southwest tapering edge of the FTC is acoustically transparent (blank) or possess weakly developed reflectors (Figs. 8 and 9) consistent with these sediments representing either mass flows deposited as the ice retreated and/or indicating that they have been highly deformed adjacent to what would have been a gently W/SW-dipping ice-contact slope.

To the west/southwest of the FTC is a basin (70-100 m deep) filled by an essentially undeformed sequence which thins (onlaps) onto the western margin of the glacitectonic complex and may, at least in part, be equivalent to the upper DBF (Figs. 4 and 9). However, due to the absence of boreholes in this area the sedimentary characteristics of this sequence remain uncertain. The comparable size of the basin with respect to the adjacent FTC (see Fig. 9) has led to the conclusion that it may represent the source depression for this glacitectonic complex, forming during the detached and removal of thrust-blocks of pre-existing California Glacigenic Group sediments (i.e. the hole of a glacitectonic hill-hole-pair). Variation in the acoustic properties on the seismic profiles reveal that the resulting basin was infilled by several laterally extensive to lenticular sedimentary units separated by erosion surfaces (Figs. 4 and 9). The upper part of the sequence is locally incised by several lenticular channel-like

features (Fig. 9). On seismic profiles 6 and 7 (Fig. 4b, c, respectively) the sediments filling the basin are interrupted by a narrow (1.0-1.5 km wide) ridge-like feature composed of acoustically blank, possibly deformed sediments, and interpreted as a possible recessional moraine.

The FTC and underlying pre-DBF California Glacigenic Group sequence are deformed by several steeply inclined, NE-directed reverse faults which are marked by an acoustically blank to semi-transparent zone possessing a distinctive 'streaked' appearance on the seismic profiles (Fig. 8). These faults locally offset (postdate) the basal décollement to this glacitectonic complex, as well as disrupt the upright folds within the FTC (Figs. 4, 8 and 10). Importantly, reflectors within the lower part of the FTC, and underlying Californian Glacigenic Group succession, show very little vertical offset across the high-angle faults suggesting that displacement on these structures may have been predominantly strike-slip.

4.4. Area C: evidence of a break/breach in the TBM complex

In contrast to the glacitectonised sequences in areas A and B, the subsurface geology in Area C (seismic profiles 11–13, Fig. 2) is dominated by a thick sequence (20-40 m thick) of essentially undeformed upper DBF overlying a typically thin (≤15 m thick) deformed unit (Fig. 5). The relative intensity and complexity of deformation within the lower DBF in Area C is much lower than in the other areas (compare Fig. 5 with Figs. 2b and 4). Furthermore, the cross-sections (Fig. 5) and horizon map (Fig. 2) indicate that Area C lacks the large ridge-like thrust-block moraines which characterise the other areas. The gently undulating upper surface to the lower DBF is marked by a band of bright reflectors and therefore interpreted as a desiccation surface which was exposed for a prolonged period prior to the deposition of the overlying upper DBF. The erosive base of the upper DBF locally dissects this palaeo-land surface, cutting downward into the underlying deformed sediments. Well-developed reflectors on the seismic profiles indicate that the upper DBF is moderately to well-bedded, and comprises several tabular, laterally extensive sediment packages separated by erosion surfaces, as well as several large (2-5 km across, ≤10-20 m deep), approximately N-S-trending channels (Figs. 2 and 5). Bands of bright reflectors within the upper DBF are once again thought to record significant breaks in sedimentation.

The laterally extensive nature of the upper DBF sediment packages is consistent with their deposition in a wide (15-30 km across), northeast to southwest-tending basin (LB2 on Fig. 2) which underlies most of Area C. The horizon map shown on Fig. 2a clearly indicates that this basin crosscuts the thrust-block moraines which characterise the subsurface geology of the adjacent areas (also see Fig. 3b). Consequently, this basin is thought to represent a significant breach within the glacitectonic landsystem underlying the western part of Dogger Bank (Fig. 2b). The origin of this "breach" is uncertain, with the erosional base of the upper DBF sequence indicating that it post-dates the thrust-

329 block moraines and is therefore itself erosional. Alternatively, it may have exploited a topographic low
330 within the thrust-block moraines where these glacitectonic landforms were less well-developed
331 enabling meltwater to break through the topographically higher moraines located to the north (Area
332 A) and south (Area B) (Fig. 2b, also see 14) leading to the deposition of the laterally extensive upper
333 DBF which characterises Area C.

334

335 ## 5. The relationship between the TBM and FTC in Area B

336 The geological cross sections (Fig. 4) reveal that the boundary zone between the shallow W/SW-
337 directed deformation associated with the thrust-block moraines (TBM), and the deep-seated E/NE-
338 directed fold and thrust complex located along the western margin of Dogger Bank, is overlain by a
339 10-40 m thick sequence of variably deformed upper DBF sediments which in general thickens towards
340 the southwest (Figs. 8, 11 and 12). Variation in the acoustic properties within the upper DBF indicates
341 that it comprises a number of lenticular sedimentary packages separated by undulating to irregular
342 erosion surfaces and incised by deep (up to 60 m) channels (Fig. 11). Correlation between the cross-
343 sections through this boundary zone reveal that these sediments were deposited in an elongate basin
344 which is *c*. 5-7 km wide in the north (Fig. 6a, b), narrowing to 2-3 km or even absent (Fig. 6c, d), before
345 widening once again to *c*. 7-8 km wide further to the south (Fig. 6e, g). The base of the upper DBF
346 within this basin locally appears to truncate the folds and thrusts within the underlying glacitectonised
347 sequences (Figs. 8, 11 and 12). Elsewhere, however, these structures propagate upwards to deform
348 the lower parts of this sedimentary sequence, indicating that glacitectonism was
349 penecontemporaneous with at least the earlier stages of sedimentation within the basin. The lower
350 parts of the sedimentary subunits identified on the northeast-side of the basin, thin toward both the
351 northeast and southwest (Figs. 11 and 12), consistent with their deposition as a series of fans or aprons
352 formed along the leading edge of the TBM and associated ice sheet margin located to the
353 east/northeast.

354 The cross-sections also reveal that the relationship between the two glacitectonic complexes changes
355 along strike (Fig. 4). On most of the seismic profiles, the leading edge of the FTC (corresponding to the
356 structurally lower domain; Fig. 8) extends north-eastwards where it structurally underlies the western
357 most limit of the TBM which is composed of SW-directed folded and thrust lower DBF (Figs. 4, 8 and
358 11). This relationship suggests that the deep-seated, NE-directed thrusting and folding along the
359 western margin of Dogger Bank predated the glacitectonism observed elsewhere within areas A and
360 B. On a small number of cross-sections, however, the relationships between the FTC and TBM are
361 more complex with these deformed sequences apparently being tectonically interleaved (Figs. 4b, f,

h and 10). For example, on seismic profile 10 (Fig. 10) the leading edge of the TBM is overridden by the structurally higher domain of the FTC with the geometry of structures within this thrust and fold complex recording NE-directed deformation (also see Fig. 4b, h). Therefore, deformation within structurally higher parts of the FTC appears to post-date the development of the southwest leading-edge of the TBM landsystem. This relatively younger phase of NE-directed glacitectonism is also thought to have resulted in the penecontemporaneous deformation of the upper DBF sediments deposited within the sedimentary basin separating these two glacitectonic complexes. Consequently, the FTC was formed as a result of two separate ice advances from the west/southwest, separated by much shallower deformation in response to the advance of ice across Dogger Bank from the north/northeast.

6. Evidence of ice-lobe interaction of the western side of Dogger Bank

It is clear that large scale glacitectonism recognised within the shallow subsurface of the western part of Dogger Bank is related to two apparently separate ice masses (Fig. 13): (i) firstly the Dogger Bank lobe which advanced from the north and was responsible for the construction of a series of arcuate thrust-block moraines (TBM) separated by topographically low-lying sedimentary basins formed during the active retreat of this ice mass (c.f. Phillips et al., 2018); and (ii) a second ice mass from the west which was responsible for the formation of the deep-seated, E/NE-directed fold and thrust complex (FTC) along the western margin of Dogger Bank. Cotterill et al. (2017a) suggested, based upon unpublished sediment provenance data, that Dogger Bank was in overridden by the FIS from the north. The western ice mass, however, is most likely to have been the North Sea lobe of the BIIS which is widely regarded to have extended into this part of the southern central North Sea during the Late Devensian (Figs. 1 and 13) (*e.g*. Jansen et al., 1979; Clark et al., 2004; Carr et al., 2006; Brooks et al., 2009; Hubbard et al., 2009; Evans et al., 2021); its maximum offshore extent being equated with the distribution of the Bolders Bank Formation (see Fig. 13) (Jansen et al., 1979; Cameron et al., 1992; Dove et al., 2017). The North Sea lobe was fed by ice from the Firth of Forth that flowed southwards through the North Sea Basin broadly parallel to the contemporary coastline of eastern England (Roberts et al., 2019; Evans et al., 2021, and references therein). Tills attributed to this ice lobe occur onshore flanking the coastlines of Northumberland, Yorkshire, Lincolnshire and north Norfolk (Catt, 2007; Davies *et al*., 2012; Evans *et al*., 2019), and possess distinctive lithological indicators that have enabled ice flow paths to be accurately reconstructed and linked to bedrock sources (Davies et al., 2012; Busfield et al., 2015; Sutherland et al., 2020). Sedimentological, structural and landform evidence demonstrates that in Yorkshire and the adjacent offshore area, forward motion of the North Sea lobe was strongly influenced by subglacial deformable beds (Evans et al., 1995; Evans and

Thomson, 2010; Dove et al., 2017). This facilitated the development a piedmont-style ice margin (Dove et al., 2017) with local ice-marginal behaviour controlled by variations in sediment rheology and porewater availability (Sutherland et al., 2020). Much of the western- (East Yorkshire, Lincolnshire) and southernmost (north Norfolk) onshore extent of this ice lobe coincides with limestone (chalk) bedrock which formed relatively elevated areas of the landscape (Bateman et al., 2015). The elevated permeability of the limestone bedrock combined with the reverse gradient acted to enhance ice-bed traction by removing water from the subglacial bed, thereby generating sticking points and the development of a more permanent ice-marginal position.

Further to the north and east, the topographic high represented by Dogger Bank would have influenced the flow and expansion of the North Sea lobe to the west (c.f. Dove et al., 2017). The complex relationships between the TBM and FTC (Figs. 10 to 12) are interpreted as recording the interaction of the North Sea and Dogger Bank lobes along the western side of Dogger Bank, with this area eventually being inundated by ice advancing from the north (Cotterill et al., 2017, Phillips et al., 2018). The cross-sections through the western part of Dogger Bank (Figs. 4, 11 and 12) reveal that the earlier phase of NE-directed thrusting and folding within FTC, predated the formation of the TBM associated with the advance and, at least the initial stages, of the active retreat of the Dogger Bank lobe. It is possible that the evolving FTC formed a topographic barrier along the western margin of Dogger Bank which restricted the subsequent westerly expansion of the Dogger Bank lobe (Figs. 13 and 14). The structurally complex zone separating the two evolving glacitectonic landsystems was progressively buried by sediments deposited by a series of fans/aprons prograding into an elongate, approximately N-S-trending marginal basin which formed between the North Sea and Dogger Bank lobes (Fig. 14). The lack of a significant west-derived component in this sedimentary fill further suggests that the FTC may have formed a topographic barrier which also influenced the pattern of sedimentation within the evolving marginal basin. Oscillation of the margin of the North Sea lobe, comparable to that observed along the east coast of England (cf. Dove et al., 2017; Evans et al., 2021), may have resulted in the retreat of this ice mass from the western side of Dogger Bank. As it retreated from its marginal position represented by the FTC and into the source depression located to the west/southwest, it would have further increased the impact of this large glacitectonic landform by potentially preventing meltwater and sediment being released from this westerly ice mass to drain east/northeast wards into the evolving ice-marginal basin (Fig. 14).

The tectonic interleaving of the FTC and TBM (Fig. 10) indicates that at some point the North Sea lobe readvanced leading renewed construction of the FTC, as well as deformation of the sediments being deposited within the marginal basin formed between the two ice masses. Consequently, deep-seated glacitectonism along the western margin of Dogger Bank is thought to record at least two phases of

advance of the North Sea lobe from the west, separated by the much shallower deformation resulting from the advance and subsequent active retreat of the Dogger Bank lobe to the north (Fig. 14). The eventual retreat of the North Sea lobe would have revealed the large source depression to the FTC which was then filled by a thick sequence of glacial and possibly post-glacial sediments (Fig. 9).

7. Glacitectonism and sedimentation associated with active retreat of the Dogger Bank ice

The W/SW-directed glacitectonism which dominates the shallow subsurface structure across most of the western part of Dogger Bank (areas A and B, Fig. 2) is consistent with these thrust-block moraines (TBM 1 to 4; Figs. 2b and 14) having formed in response to ice-marginal to proglacial deformation associated with the active retreat of the Dogger Bank lobe (Fig. 14), possibly forming the western edge of the FIS (c.f. Phillips *et al*., 2018). Although these glacitectonic landforms have locally been modified by erosion which accompanied the deposition of the overlying upper DBF, and truncated at the base of the Holocene and/or seabed sediments (Figs. 3 and 4), there is no evidence to suggest that they were overridden during a later advance. Consequently this buried glacitectonic landsystem records the complex interplay between glacitectonism and penecontemporaneous ice-marginal to proglacial sedimentation during the active retreat of highly dynamic ice sheet margin during the deglaciation of the western Dogger Bank (Fig. 14) (c.f. Phillips et al., 2018).

Changes in structural style and relative intensity of deformation within the individual thrust-block moraines indicates that the Dogger Bank lobe repeatedly reoccupied the same ice limit during this active retreat, initially leading to the construction of large (15-20 km wide), arcuate moraine system which dominates much of Area A (TBM 1 and 2; Fig. 14). Mapping of the buried thrust-block moraines reveals that they occur in three principal groups (Fig. 2), suggesting that they may record three significant periods of ice sheet readvance during deglaciation (readvance phases A, B and C on Fig. 14). The complexity of TBM1 and 2, clearly indicates that the Dogger Bank lobe reoccupied this limit over an extended period, leading to the conclusion that this landform assemblage probably represents a significant period of still-stand during deglaciation which may have occurred relatively shortly after the ice sheet had retreated from its maximum limit located further to the south/southeast. In contrast, the relatively smaller, internally less complex, TBM3 and TBM4 landform assemblages may represent shorter periods of readvance. The decrease in size and complexity of the thrust-block moraines northwards across the western Dogger Bank (TBM 1 to 4; Fig. 14) is, therefore, considered to reflect a reduction in the magnitude/scale of successive phases of readvance during deglaciation, reflecting a decrease in the dynamics of the ice sheet during the deglaciation of Dogger Bank.

The closely spaced nature of the thrust-block moraines within Area B (Fig. 2) is consistent with this area occupying a more lateral-marginal position with respect to the lobate margin of the Dogger Bank lobe (see Fig. 14). However, the upper DBF filling within the intervening basins comprises a similar tripartite sequence (Fig. 4) to that observed further to the south in areas A (Fig. 3) and C (Fig. 5). This sequence can be subdivided into: (i) a lower sequence composed of lenticular sediment packages laid down by fans/aprons which prograded into the basins from the adjacent moraines; (ii) overlain by laterally extensive, tabular outwash deposits possibly laid down by braided meltwater channels; and (iii) an upper channelised sequence which is incised into the underlying deposits, recording the establishment of a more stable drainage system during ice sheet retreat (Fig. 14). Desiccation surfaces (bands of bright reflectors) within the upper Dogger Bank are considered to represent significant breaks in sedimentation and periods of subaerial exposure due to either a change in the pattern of drainage within the forefield of the retreating ice sheet, and/or a decrease in meltwater production during periods of ice sheet readvance. The approximately N-S-trending channels within the ice-marginal basins in Area B appear to flow into the north-side of the large (15-30 km across), NE-SW-trending basin underlying Area C (LB2; Figs. 2 and 14). This basin is thought to have represented a significant breach (or break) within the glacitectonic (TBM) landsystem (Fig. 14) and is infilled by laterally extensive units of upper DBF sediments incised by large (2-5 km across) N-S-trending channels (Fig. 5). These channels are considered to have formed a stable drainage system within the forefield of the retreating ice sheet (Fig. 14) and would have precluded the development of a large proglacial lake within this part of Dogger Bank. However, a relatively large (750 km^2) proglacial lake, but much smaller than predicted by previous studies (*e.g*. Cameron et al., 1992; Clarke et al., 2012; Hijma et al., 2012; Cohen et al., 2014; Sejrup et al., 2016; Hjelstuen et al., 2017), has been identified to the east of the present study area (Cotterill et al., 2017a; Emery et al., 2019). Emery et al. (2019) demonstrated that this lake was dammed to the east by a large thrust-block moraine and was progressively infilled by a sequence (≤30 m thick) of glacial outwash (upper DBF) and lacustrine sediments. The presence of this proglacial lake would have had a marked impact on the nature of the ice sheet margin and its style of retreat which would have contrasted markedly with active retreat history preserved within the DBF underlying the western Dogger Bank.

8. Implications for Late Devensian ice sheet evolution on Dogger Bank

The timing of the initial inundation of Dogger Bank by ice during the last glaciation has historically been poorly constrained (Sejrup et al., 2000; Carr et al., 2006; Clark et al., 2012; Hughes et al., 2016). However, this has recently been constrained to around 30-29 ka BP by geochronology with North Sea lobe reaching its maximum extent by around 27 ka BP (Roberts et al., 2018; Evans et al., 2021). Dating

of proglacial lake deposits located to the north of Dogger Bank by Roberts et al. (2018) indicate that ice retreated rapidly from the area prior to 23 ka BP (also see Evans et al., 2021), rather than the much later date of 18.5 ka BP initially proposed by Clark et al. (2012) and Sejrup et al. (2016). As previously noted, the southern limit of the Late Devensian (Weichselian) ice sheet(s) in the North Sea is as yet poorly constrained (Fig. 1; also see fig. 3 of Phillips et al., 2017). Although Cameron et al. (1992) argued that the maximum ice limit lay to the north and west of Dogger Bank, several recent studies present clear evidence that the ice sheet did in fact extend across the area (Cotterill et al., 2017a; Phillips et al., 2018; Roberts et al., 2018; Emery et al., 2019). However, the precise maximum limit of the Dogger Bank lobe remains uncertain. Data presented here clearly indicates that the deformed lower DBF extends to the south and east of the present study area, indicating that the maximum limit of the ice sheet lay further to the south (see Fig. 13). Emery et al. (2019) inferred, based upon the lack of evidence for glacial advance (*e.g.* moraines) in the Oyster Ground (Fig. 13) and thickening of Late Holocene sands, that the ice sheet did not extend beyond the break of slope marking the southeast margin of Dogger Bank.

The present study demonstrates that ice sheet dynamics across Dogger Bank were far more complex than previously thought (*e.g*. Carr et al., 2006; Graham et al., 2011) and involved the interaction between the North Sea lobe of the BIIS, which advanced from the west, with a highly dynamic Dogger Bank lobe which expanded and subsequently retreated to the north/northwest (Fig. 13). Prior to the Late Devensian, Dogger Bank was already considered to represent a topographic high within the southern central North Sea basin, composed of shallow, northward prograding marine sands (Cameron et al., 1992; Cotterill et al., 2017a) which formed a gently N/NW-dipping (adverse) slope in front of the advancing ice sheets. The first ice mass to impinge on the topographic high formed by Dogger Bank from the north was the North Sea lobe as it expanded south and eastwards into this part of the North Sea. It is likely that the reverse slope formed by the western margin of Dogger Bank led to an increased coupling of the ice sheet to its bed, resulting in the transfer of stresses into the underlying Californian Glacigenic Group sequence, leading to the observed deep-seated glacitectonic deformation (FTC). Previous ice sheet reconstructions have demonstrated that the BIIS flowed southward around the western side of Dogger Bank (*e.g.* Jansen et al., 1979; Clarke et al., 2004; Carr et al., 2006; Brookes et al., 2009; Dove et al., 2017; Evans et al., 2021), eventually extending into the Humber, Wash and Outer Silver Pit areas (Figs. 1 and 13) and reaching its maximum extent between 25.8–24.6 ka (Evans et al., 2021). If correct, it suggests that the FTC on the western margin of Dogger Bank initially occupied a frontal marginal position during the earlier expansion of the North Sea lobe, changing to a more lateral ice-marginal position as the North Sea lobe extended southwards (Figs. 13 and 14). Oscillation of this ice margin would have led to the repeated accretion of detached thrust-

blocks of pre-existing Californian Glacigenic Group sediments onto the western (up-ice) margin of the evolving deep-seated FTC. The progressive development of this glacitectonic landform was therefore accompanied by the excavation of the large source depression located immediately to the west (Fig. 9), leading to a further steepening of the west/northwest margin of Dogger Bank. This glacitectonic modification of the morphology of the western margin of Dogger Bank may also have been partially responsible for limiting the eastward expansion of the North Sea lobe, thereby influencing the change to a more southerly direction of flow. This would have been amplified by the presence within the subglacial bed to the west of Dogger Bank of saturated pre-existing Quaternary sediments and/or Jurassic mudrocks that would have facilitated subglacial deforming beds and fast ice flow (Figs. 13 and 14).

The change to a more lateral ice-marginal position of the FTC will have resulted in a significant change in the orientation of the stress regime responsible for glacitectonism; from E-directed compression responsible for large-sale folding and thrusting within the evolving FTC, to a transpressional regime involving components of strike-slip and compressional deformation. Possible evidence for this change may be provided by the high-angle reverse (compressional) and postulated strike-slip faults which offset the earlier formed folds and thrusts within the FTC, with this late-stage faulting occurring as the North Sea lobe flowed southward to bypass Dogger Bank (Figs. 13 and 14). Dove et al. (2017) demonstrated that the subsequent retreat of the North Sea lobe from this part of the southern North Sea was punctuated by several phases of readvance resulting in the formation of a series of broad sedimentary wedges and associated moraines. Roberts et al. (2018) presented age data which indicated that the expansion of the North Sea lobe to the south of Dogger Bank had occurred by 29–30 ka (also see Evans et al., 2021). This is consistent with the complex structural relationships displayed between the FTC and TBM which indicate that the North Sea lobe of the BIIS already occupied a position to the west/southwest of Dogger Bank prior to it being inundated by ice from the north (Fig. 15). The large glacitectonic landform associated with the construction of the FTC is believed to have formed a prominent topographic barrier which may have restricted the subsequent westerly expansion of the Dogger Bank lobe confining its maximum limit in this area to the edge of the present-day Dogger Bank (Figs. 13 and 14).

As described above, during deglaciation the highly dynamic Dogger Bank lobe underwent active retreat leading to a complex interplay between glacitectonism and penecontemporaneous proglacial sedimentation (Fig. 14) (Phillips et al., 2018). In western Canada, the construction of comparable regionally extensive glacitectonic landsystems (Neutral Hills, Sharp Hills, Misty Hills, Mud Buttes) have been associated with the surge-like activity within the Prospect Valley lobe of the Central Alberta Ice Stream during the northward retreat of the Laurentide Ice Sheet (Evans et al., 2008, 2014; O'Cofaigh

et al., 2010; Atkinson et al., 2014; Phillips et al., 2017; Evans et al., 2018), providing an analogue and hence support for linking large-scale glacitectonism on western Dogger Bank to fast ice flow (Phillips et al., 2018). The potential for fast ice flow from the north/northwest across Dogger Bank was also indicated by the model simulations of Boulton and Hagdorn (2006) and the reconstruction for the Late Devensian/Weichselian ice sheet within the North Sea basin of Sejrup et al. (2016). Both studies suggest that during the last glaciation the BIIS (Devensian) and FIS (Weichselian) were confluent forming a single ice mass and that during the initial stages of collapse, ice inundating Dogger Bank would have been flowing south/south-southeast from an approximately E-W-trending ice divide linking northeast Scotland and southern Norway (see fig. 10 of Boulton and Hagdorn, 2006 and fig. 3 of Sejrup et al., 2016). The low basal shear stresses equated with fast ice flow (ice streaming) may have enabled the Dogger Bank lobe to ride up the reverse slope forming the northern margin of this topographic high. A similar model involving fast ice flow during the initial expansion of ice across Dogger Bank was subsequently suggested by Emery et al. (2019). However, in contrast to western Dogger Bank, the ice which inundated this more eastern area underwent a markedly different style of retreat.

A large thrust-block moraine identified by Emery et al. (2019) as marking the maximum limit of the Dogger Bank ice, to the east of the present study area, dammed a large (*c*. 750 km^2) proglacial lake which formed as the ice sheet retreated northward (also see Cotterill et al., 2017a). It is possible that this moraine may represent a lateral extension of the TBM1/2 and, therefore, the actual maximum limit of the Dogger Bank lobe lay further to the east/southeast. Emery *et al*. interpreted the rhythmically laminated sediments within the distal parts of the lake as varves, arguing that this lake may have existed for *c*. 1500-2000 years. In contrast to land-terminating ice sheets, the retreat of water (lake)-terminating glaciers will be strongly influenced by conditions at the glacier-lake boundary (*e.g*. thermally induced melting leading to thinning of the ice margin) which can directly affect the rate of calving activity which can lead to an enhanced rate of retreat (Van der Veen, 2002; Benn et al., 2007; Carrivick and Tweed, 2013). Furthermore, where a glacier terminates in deeper water it may begin to float reducing the effective pressure at the ice-bed interface, which can lead to an increase in glacier velocity and longitudinal extension making it more vulnerable to fracturing and calving (Van der Veen, 2002; Benn et al., 2007).

The depth of the lake on Dogger Bank is, however, unknown. Desiccation surfaces within this undeformed lacustrine sequence may indicate that it was relatively shallow, draining on a number of occasions and exposing the lakebed to periods of drying (Cotterill et al., 2017a; Emery et al., 2019). Previous studies (Cotterill et al., 2017a; Emery et al., 2019) have suggested that the periodic draining of the lake may have occurred to the east via a deeply incised (50-60 m deep) outflow channel cutting

599 through the thrust-block moraine which formed the dam. The complex sequence of sediments infilling
600 the channel were interpreted as recording the repeated catastrophic draining of the lake by glacial
601 outburst floods (Cotterill et al., 2017a). However, once the moraine damming the lake had been
602 breached it is difficult to envisage how it was able to repeatedly refill. Alternatively, the lowering of
603 the water level in the lake may have been controlled by changes in meltwater supply, for example due
604 to a marked change, or reconfiguration in the pattern of englacial/subglacial drainage during the
605 periodic readvance (active retreat) of the ice sheet margin. Emery et al. (2019) concluded that the lake
606 eventually became isolated from the retreating ice-sheet margin leading to a slowing of the rate of
607 retreat of the Dogger Bank lobe in this eastern area. However, subsequent retreat of the ice sheet
608 from Dogger Bank after the Late Devensian (at *c*. 27 ka) may have been relatively rapid due to the N-
609 dipping negative slope formed by the underlying California Glacigenic Group sequence.

610

611 ## 9. Conclusions

612 High-resolution seismic data from the western side of Dogger Bank obtained during a major offshore
613 windfarm development are used to demonstrate that ice sheet dynamics across the area were far
614 more complex than previously thought, and involved the BIIS, advancing from the west, interacting
615 with the Dogger Bank lobe of the FIS expanding from the north. The complex structural relationships
616 between the thrust-block moraines (TBM) and fold and thrust complex (FTC) indicates that these ice
617 masses interacted along the western-side of Dogger Bank, with its inundation by ice probably
618 occurring during the last glaciation when both the BIIS (Devensian) and FIS (Weichselian) attained their
619 maximum extents. The impact of the North Sea lobe of the BIIS was restricted to the western margin
620 of Dogger Bank where it formed a deep-seated, E/NE-directed fold and FTC. The FTC initially occupied
621 a frontal marginal position during the earlier stages of expansion of the North Sea lobe, changing to a
622 more lateral ice-marginal position as the ice sheet continued to expand towards the south. The highly
623 dynamic Dogger Bank lobe underwent active retreat leading to a complex interplay between
624 glacitectonism and penecontemporaneous proglacial sedimentation, and the construction of a
625 complex system TBM separated by low-lying basins filled by glacigenic outwash. A NE-SW-trending
626 break or breach within the glacitectonic landsystem, filled by laterally extensive outwash sediments,
627 is considered to have allowed meltwater to drain away from the retreating ice sheet margin. Draining
628 of the forefield to the Dogger Bank lobe was also facilitated by a number of large, deeply incised
629 channels filled by a complex sequence of sediments indicating that they were active over a prolonged
630 period. The structurally complex zone separating the FTC and TBM systems was buried by sediments
631 deposited as a series of fans or aprons which prograded from the north/northeast into an elongate
632 basin which formed between the two ice masses. In contrast to the active retreat history of the

western part of the Dogger Bank lobe, the formation of a large proglacial lake further to the east resulted in this part of the ice sheet undergoing a very different style of retreat.

10. Acknowledgements

The authors would like to thank the Forewind Consortium (Equinor, Statkraft, RWE and SSE) for their permission to use the 2D seismic data acquired during surveys conducted for licensing purposes. Jonathan Lee (BGS) is thanked for his constructive review and comments on an earlier version of this paper. Jim Rose and Claire Mellett are thanked for their very positive reviews of this paper. In addition we thank colleagues at the Norwegian Geotechnical Institute and RPS Energy including Leo James, Carl Fredrik Forsberg, Tor Inge Yetginer-Tjelta, Tom Lunne, Don de Groot, Oyvind Blaker and Callum Duffy. This paper is published with permission of the Director of the British Geological Survey and Equinor/SSE.

11. References

Andersen, L.T., Hansen, D.L., Huuse, M. 2005. Numerical modelling of thrust structures in unconsolidated sediments: implications for glaciotectonic deformation. Journal of Structural Geology 27, 587–596.

Atkinson, N., Utting, D.J., Pawley, S.P. 2014. Landform signature of the Laurentide and Cordilleran ice sheets across Alberta during the last glaciation. Canadian Journal of Earth Sciences 51, 1067–1083.

Bakker, M.A.J., van der Meer, J.J.M. 2003. Structure of a Pleistocene push-moraine revealed by ground-penetrating radar: the eastern Veluwe Ridge, the Netherlands. In: Bristow, C.S., Jol, H.M. (Eds.), Ground Penetrating Radar in Sediments. Geological Society, London, Special Publications, 211, 143–151.

Balson, P.S., Cameron, T.D.G. 1985. Quaternary mapping offshore East Anglia. Marine Geology 9, 221–239.

Bateman, M.D., Evans, D.J.A., Buckland, P.C., Connell, E.R., Friend, R.J., Hartmann, D., Hartmann, D., Moxon, H., Fairburn, W.A., Panagiotakopulu, E., Ashurst, R.A. 2015. Late glacial dynamics of the Vale of York and North Sea lobes of the British and Irish Ice Sheet. Proceedings of the Geologists' Association 126, 712–730.

662 Beets, D.J., Meijer, T., Beets, C.J., Cleveringa, P., Laban, C., van der Spek, A.J.F. 2005. Evidence for a
663 Middle Pleistocene glaciation of MIS 8 age in the southern North Sea. Quaternary International 133-
664 134, 7–19.

665 Belt, T. 1874. An examination of the theories that have been proposed to account for the climate of
666 the glacial period. Quarterly Journal of Science, 421–464.

667 Benn, D.I., Evans, D.J.A. 2010. Glaciers and Glaciation. Arnold, London, U. K. 802 pp.

668 Benn, D.I., Warren, C.R., Mottram, R.H. 2007. Calving processes and the dynamics of calving glaciers.
669 Earth-Science Reviews, 82(3–4), 143–179 (doi: 10.1016/j.earscirev.2007.02.002)

670 Bluemle, J.P., Clayton, L. 1983. Large-scale glacial thrusting and related processes in North Dakota.
671 Boreas 13, 279–299.

672 Boulton, G.S., Caban, P. 1995. Groundwater flow beneath ice sheets, part II; Its impact on glacier
673 tectonic structures and moraine formation. Quaternary Science Reviews 14, 563–587.

674 Boulton, G.S., Hagdorn, M. 2006. Glaciology of the British Isles Ice Sheet during the last glacial cycle:
675 Form, flow, streams and lobes. Quaternary Science Reviews 25, 3359–3390.

676 Böse, M., C Lüthgens, C., JR Lee, J.R., Rose, J. 2012. Quaternary glaciations of northern Europe.
677 Quaternary Science Reviews 44, 1–25.

678 Bradwell, T., Stoker, M.S., Golledge, N.R., Wilson, C.K., Merritt, J.W., Long, D., and others. 2008. The
679 northern sector of the last British Ice Sheet: maximum extent and demise. Earth Science Reviews 88,
680 207–226.

681 Bradwell, T., Sigurdsson, O., Everest, J. 2013. Recent, very rapid retreat of a temperate glacier in SE
682 Iceland. Boreas 42, 959–973.

683 British Geological Survey and Rijks Geologische Dienst. 1989. Silver Well Quaternary Geology. 1:250
684 000. Keyworth, Nottingham: British Geological Survey.

685 British Geological Survey and Rijks Geologische Dienst. 1991. Dogger Quaternary Geology. 1:250 000.
686 Keyworth, Nottingham: British Geological Survey.

687 Brooks, A.J., Bradley, S.L., Edwards, R.J., Milne, G.A., Horton, B., Shennan, I. 2008. Postglacial relative
688 sea-level observations from Ireland and their role in glacial rebound modelling. Journal of Quaternary
689 Science 23, 175–192.

690 Burke, H., Phillips, E., Lee, J.R., Wilkinson, I.P. 2009. Imbricate thrust stack model for the formation of
691 glaciotectonic rafts: an example from the Middle Pleistocene of north Norfolk, UK. Boreas 38, 620–
692 637.

693 Cameron, T.D.J., Stoker, M.S., Long, D. 1987. The history of Quaternary sedimentation in the UK sector
694 of the North Sea Basin. Journal of the Geological Society, London 144, 43–58.

695 Cameron, T.D.J., Crosby, A., Balson, P.S., Jeffery, D.H., Lott, G.K., Bulat, J., Harrison, D.J. 1992. United
696 Kingdom offshore regional report: the geology of the southern North Sea. London: HMSO for the
697 British Geological Survey.

698 Carr, S.J., Holmes, R., van der Meer, J.J.M., Rose, J. 2006. The Last Glacial Maximum in the North Sea
699 Basin: micromorphological evidence of extensive glaciation. Journal of Quaternary Science 21, 131–
700 153.

701 Carrivick, J.L., Tweed, F.S. 2013. Proglacial lakes: character, behaviour and geological importance.
702 Quaternary Science Reviews 78, 34–52 (doi:10.1016/j.quascirev.2013.07.028)

703 Caston, V.N.D. 1977. A new isopachyte map of the Quaternary of the North Sea. Institute of Geological
704 Sciences Report 10 (11), 3–10.

705 Caston, V.N.D. 1979. The Quaternary sediments of the North Sea. In: Banner, F.T., Collins, M.B.,
706 Massie, K.S. (eds) The North-West European shelf seas: The sea bed and the sea in motion. 1. Geology
707 and Sedimentology. Elsevier, New York. 195–270.

708 Catt, J.A. 1991. Late Devensian glacial deposits and glaciations in eastern England and the adjoining
709 offshore region. In: Ehlers J, Gibbard PL, Rose J (eds) Glacial Deposits in Great Britain Ireland. A.A.
710 Balkema: Rotterdam. 61–68.

711 Catt, J.A. 2007. The Pleistocene glaciations of eastern Yorkshire: a review. Proceedings of the Yorkshire
712 Geological Society 56, 177–207.

713 Cohen, K.M., Gibbard, P.L., Weerts, H.J.T. 2014. North Sea palaeogeographical reconstructions for the
714 last 1 Ma. Geologie en Mijnbouw 93, 7–29.

715 Cotterill, C.J., Phillips, E., James, L., Forsberg, C.F., Tjelta, T.I. 2017a. How understanding past
716 landscapes can inform present day site investigations: A case study from Dogger Bank, southern
717 central North Sea. Near Surface Geophysics 15, 403–413.

718 Cotterill, C.J., Phillips, E., James, L., Forsberg, C.F., Tjelta, T.I., Dove, D. 2017b. The evolution of the
719 Dogger Bank, North Sea: a complex history of terrestrial, glacial and marine environmental change.
720 Quaternary Science Reviews 171, 136–153.

721 Clark, C.D., Evans, D.J.A., Khatwa, A., Bradwell, T., Jordan, C.J., Marsh, S.H., Mitchell, W.A., Bateman,
722 M.D. 2004. Map and GIS database of glacial landforms and features related to the last British Ice Sheet.
723 Boreas 33, 359–375.

724 Clark, C.D., Hughes, A.L.C., Greenwood, S.L., Jordan, C., Sejrup, H.P. 2012. Pattern and timing of retreat
725 of the last British-Irish Ice Sheet. Quaternary Science Reviews 44, 112–146.

726 Davies, B.J., Roberts, D.H., Bridgland, D.R., Ó Cofaigh, C. 2012. Dynamic Devensian ice flow in NE
727 England: a sedimentological reconstruction. Boreas 41, 337–366

728 Davis, D., Suppe, J., Dahlen, F.A. 1984. Mechanics of fold-and-thrust belts and accretionary wedges:
729 Cohesive Coulomb theory. Journal of Geophysical Research 89, 10087–10101.

730 Dove, D., Evans, D.J.A., Lee, J.R., Roberts, D.H., Tappin, D.R., Mellett, C.L., Long D., Callard, V.L. 2017.
731 Phased occupation and retreat of the Last British-Irish Ice Sheet in the southern North Sea;
732 geomorphic and seismostratigraphic evidence of a dynamic ice lobe. Quaternary Science Reviews 163,
733 114–134.

734 Dunlop, P., Shannon, R., McCabe, M., Quinn, R., Doyle, E. 2010. Marine geophysical evidence for ice
735 sheet extension and recession on the Malin Shelf: New evidence for the western limits of the British
736 Irish Ice Sheet. Marine Geology 276, 86–99.

737 Eisma, D., Jansen, J.H.F., van Weering, T.C.E. 1979. Sea floor morphology and recent sediment
738 movement in the North Sea. In: Oele, E., Schuttenhelm, R.T.E., Wiggers, A.J. (eds) The Quaternary
739 history of the North Sea. Acta Univ. Ups. Symposium. Univ. Ups Annum Quintegentesimum
740 Celebrantis, Uppsala. 217–231.

741 Ehlers, J., 1990. Reconstructing the dynamics of the north-west European Pleistocene ice sheets.
742 Quaternary Science Reviews 9, 71–83.

743 Evans, D.J.A., Thomson, S.A. 2010. Glacial sediments and landforms of Holderness, eastern England: a
744 glacial depositional model for the North Sea Lobe of the British-Irish Ice Sheet. Earth Science Reviews
745 101, 147–189.

746 Evans, D.J.A., Owen, L.A., Roberts, D.H. 1995. Stratigraphy and sedimentology of Devensian
747 (Dimlington Stadial) glacial deposits, East Yorkshire, England. Journal of Quaternary Science 10, 241–
748 265.

749 Evans, D.J.A., Twigg, D.R. 2002. The active temperate glacial landsystem: a model based on
750 Breiðamerkurjökull and Fjallsjökull, Iceland. Quaternary Science Reviews 21, 2143–2177.

751 Evans, D.J.A., Clark, C.D., Rea, B.R. 2008. Landform and sediment imprints of fast glacier flow in the
752 southwest Laurentide Ice Sheet. Journal of Quaternary Science 23, 249–272.

753 Evans, D.J.A., Young, N.J., Cofaigh, C. 2014. Glacial geomorphology of terrestrial terminating fast flow
754 lobes/ice stream margins in the southwest Laurentide ice sheet. Geomorphology 204, 86–113.

755 Evans, D.J.A., Roberts, D.H., Bateman, M.D., Ely, J., Medialdea, A., Burke, M.H., Chiverrell, R.C., Clark,
756 C.D., Fabel, D. 2019. A chronology for the North Sea Lobe advance and recession on the Lincolnshire
757 and Norfolk coasts during MIS 2 and 6. Proceedings of the Geologists' Association 130, 523–540.

758 Evans, D.J.A., Roberts, D.H., Bateman, M.D., Clark, C.D. Medialdea, A., Callard, L., Grimoldi, E.,
759 Chiverrell, R.C., Ely, J., Dove, D., Ó Cofaigh, C., Saher, M., Bradwell, T., Moreton, S.G., Fabel, D., Bradley,
760 S.L. 2021. Retreat dynamics of the eastern sector of the British–Irish Ice Sheet during the last
761 glaciation. Journal of Quaternary Science 36, 723–751.

762 Gatliff, R.W., Richards, P.C., Smith, K., Graham, C.C., McCormack, M., Smith, N.J.P., Jeffery, D., Long,
763 D., Cameron, T.D.J., Evans, D., Stevenson, A.G., Bulat, J., Ritchie, J.D. 1994. United Kingdom offshore
764 regional report: the geology of the central North Sea. London: HMSO for the British Geological Survey.

765 Glennie, K.W., Underhill, J.R., 1998. Origin, development and evolution of structural styles. In: Glennie,
766 K.W. (ed.) Petroleum Geology of the North Sea: Basic Concepts and Recent Advances (fourth edition).
767 Blackwell Science Ltd., Oxford, 42–84.

768 Graham, A.G.C., Lonergan, L., Stoker, M.S. 2007. Evidence for Late Pleistocene ice stream activity in
769 the Witch Ground Basin, central North Sea, from 3D seismic reflection data. Quaternary Science
770 Reviews 26, 627–643.

771 Graham, A.G.C., Lonergan, L., Stoker, M.S. 2010. Depositional environments and chronology of Late
772 Weichselian glaciation and deglaciation in the central North Sea. Boreas 39, 471–491.

773 Graham, A.G.C., Stoker, M.S., Lonergan, L., Bradwell, T., Stewart, M.A. 2011. The Pleistocene
774 glaciations of the North Sea Basin. In: Ehlers, J., Gibbard, P.L. (eds) Quaternary Glaciations – Extent
775 and Chronology (2nd Edition), 261–278.

776 Howe, J.A. Dove, D., Bradwell, T., Gafeira, J. 2012. Submarine geomorphology and glacial history of
777 the Sea of the Hebrides, UK. Marine Geology 315-318, 64–76.

778 Huuse, M., Lykke-Andersen, H., Michelsen, O. 2001. Cenozoic evolution of the eastern Danish North
779 Sea. Marine Geology 177, 232–269.

780 Hijma, M.P., Cohen, K.M., Roebroeks, W., Westerhoff, W.E., Busschers, F.S. 2012. Pleistocene Rhine-
781 Thames landscapes: Geological background for hominin occupation of the southern North Sea: Journal
782 of Quaternary Science 27, 17–39.

783 Hubbard, A., Bradwell, T., Golledge, N., Hall, A., Patton, H., Sugden, D., Cooper, R. and Stoker, M. 2009.
784 Dynamic cycles, ice streams and their impact on the extent, chronology and deglaciation of the British-
785 Irish ice sheet. Quaternary Science Reviews, 28, 758–776.

786 Hughes, P.D., Gibbard, P.L., Ehlers, J. 2013. Timing of glaciations during the last glacial cycle; Evaluating
787 the concept of a global "Last Glacial Maximum" (LGM). Earth Science Reviews 125, 171–198.

788 Hughes, A.L.C., Gyllencreutz, R., Lohne, Ø.S., Mangerud, J., Svendsen, J.I. 2016. The last Eurasian ice
789 sheets – a chronological database and time-slice reconstruction, DATED-1. Boreas 45, 1–45.

790 Huuse, M., Lykke-Andersen, H., Michelsen, O. 2001. Cenozoic evolution of the eastern Danish North
791 Sea. Marine Geology 177, 232–269.

792 Jansen, J.H.F., van Weering, T.C.E., Eisma, D. 1979. Late Quaternary Sedimentation in the North Sea.
793 In: Oele, E., Schuttenhelm, R.T.E., Wiggers, A.J. (eds) The Quaternary history of the North Sea. Acta
794 Univ. Ups. Symposium. Univ. Ups Annum Quintegentesimum Celebrantis, Uppsala 2, 175–187

795 Kristensen, T.B., Huuse, M., Piotrowski, J.A., Clausen, O.R. 2007. A morphometric analysis of tunnel
796 valleys in the eastern North Sea based on 3D seismic data. Journal of Quaternary Science 22, 801–815.

797 Laban, C. 1995. The Pleistocene glaciations in the Dutch Sector of the North Sea. PhD Thesis,
798 Universiteit van Amsterdam, 200 pp.

799 Lee, J.R, Busschers, F.S., Sejrup, H.P. 2012. Pre-Weichselian Quaternary glaciations of the British Isles,
800 The Netherlands, Norway and adjacent marine areas south of 68°N: implications for long-term ice
801 sheet development in northern Europe. Quaternary Science Reviews 44, 213–228.

802 Lee, J.R., Phillips, E., Booth, S.J., Rose, J., Jordan, H.M., Pawley, S.M., Warren, M., Lawley, R.S. 2013. A
803 polyphase glacitectonic model for ice-marginal retreat and terminal moraine development: the
804 Middle Pleistocene British Ice Sheet, northern Norfolk, UK. Proceedings of the Geologists' Association
805 124, 753–777.

Lee, J.R., Phillips, E., Rose, J., Vaughan-Hirsch, D. 2017. The Middle Pleistocene glacial evolution of northern East Anglia, UK: a dynamic tectonostratigraphic–parasequence approach. Journal of Quaternary Science 32, 231–260.

Lonergan, L., Maidment, S.C.R., Collier, J.S. 2006. Pleistocene subglacial tunnel valleys in the central North Sea basin: 3-D morphology and evolution. Journal of Quaternary Science 21, 891–903.

Mourgues, R., Cobbold, P.R. 2006. Sandbox experiments on gravitational spreading and gliding in the presence of fluid overpressures. Journal of Structural Geology 28, 887–901.

Murton, D.K., Murton, J.B. 2012. Middle and Late Pleistocene glacial lakes of lowland Britain and the southern North Sea Basin. Quaternary International 260, 115–142.

Nieuwland, D.A., Leutscher, J.H., Gast, J. 2000. Wedge equilibrium in fold-and-thrust belts: prediction of out-of-sequence thrusting based on sandbox experiments and natural examples. Geologie en Mijnbouw 79, 81–91.

Ó Cofaigh, C., Evans, D.J.A., Smith, I.R. 2010. Large-scale reorganization and sedimentation of terrestrial ice streams during late Wisconsinan Laurentide ice sheet deglaciation. Geological Society of America Bulletin 122, 743–756.

Ottesen, D., Dowdeswell, J.A., Bugge, T. 2014. Morphology, sedimentary infill and depositional environments of the Early Quaternary North Sea Basin (56° to 62°N). Marine and Petroleum Geology 56, 123–146.

Ottesen, D., Batchelor, C.L., Dowdeswell, J.A. 2018. Morphology and pattern of Quaternary sedimentation in the North Sea Basin (52–62°N). Marine and Petroleum Geology 98, 836–859.

Pedersen, S.A.S., Boldreel, L.O. 2017. Glaciotectonic deformations in the Jammerbugt and the glaciodynamic development in the eastern North Sea. Journal of Quaternary Science 32, 183–195.

Phillips, E., Merritt, J. 2008. Evidence for multiphase water-escape during rafting of shelly marine sediments at Clava, Inverness-shire, NE Scotland. Quaternary Science Reviews 27, 988–1011.

Phillips, E., Lee, J.R., Burke, H. 2008. Progressive proglacial to subglacial deformation and syntectonic sedimentation at the margins of the Mid-Pleistocene British Ice Sheet: evidence from north Norfolk, UK. Quaternary Science Reviews 27, 1848–1871.

Phillips, E., Finlayson, A., Bradwell, T., Everest, J., Jones, J. 2014. Structural evolution triggers a dynamic reduction in active glacier length during rapid retreat: evidence from Falljökull, SE Iceland. Journal of Geophysical Research: Earth Surface 119, 2194–2208.

836 Phillips, E., Hodgson, D.M., Emery, A.R. 2017. The Quaternary geology of the North Sea Basin. Journal
837 of Quaternary Geology 32, 117–126.

838 Phillips, E., Evans, D.J.A., Atkinson, N., Kendall, A. 2017. Structural architecture and glacitectonic
839 evolution of the Mud Buttes cupola hill complex, southern Alberta, Canada. Quaternary Science
840 Reviews 164, 110–139.

841 Roberts, D.H., Evans, D.J.A., Callard, S.L., Clark, C.D., Bateman, M.D., Medialdea, A., Dove, D., Cotterill,
842 C.J., Saher, M., Ó Cofaigh, C., Chiverrell, R.C., Moreton, S.G., Fabel, D., Bradwell. T. 2018. Ice marginal
843 dynamics of the last British-Irish Ice Sheet in the southern North Sea: Ice limits timing and the influence
844 of the Dogger Bank. Quaternary Science Reviews 198, 181–207.

845 Roberts, D.H., Gromoldi, E., Callard, L., Evans, D.J.A., Clark, C.D., Stewart, H.A., Dove, D., Saher, M., Ó
846 Cofaigh, C., Chiverrell, R.C., Bateman, M.D., Moreton, S.G., Bradwell, T., Fabel, D., Medialdea, A. 2019.
847 The mixed-bed glacial landform imprint of the North Sea Lobe in the western North Sea. Earth Surface
848 Processes and Landforms 44, 1223–1258.

849 Ruszczynska-Szenajch, H. 1987. The origin of glacial rafts: Detachment, transport, deposition. Boreas
850 16, 101–112.

851 Ruszczynska-Szenajch, H. 1988. Glaciotectonics and its relationship to other glaciogenic processes. In
852 Croot, D.G. (ed.): Glaciotectonic Forms and Processes, 191–193. Balkema, Rotterdam.

853 Sejrup, H.P., Aarseth, I., Ellingsen, K.L., Reither, E., Jansen, E., Løvlie, R., Bent, A., Brigham-Grette, J.,
854 Larsen, E., Stoker, M. 1987. Quaternary stratigraphy of the Fladen area, central North Sea: a
855 multidisciplinary study. Journal of Quaternary Science 2, 35–58.

856 Sejrup, H.P., Aarseth, I., Haflidason, H., Løvlie, R., Bratten, Å., Tjøstheim, G., Forsberg, C.F., Ellingsen,
857 K.L. 1995. Quaternary of the Norwegian Channel: glaciation history and palaeoceanography.
858 Norwegian Journal of Geology 75, 65–87.

859 Sejrup, H.P., Larsen, E., Landvik, J., King, E.L., Haflidason, H., Nesje, A. 2000. Quaternary glaciations in
860 southern Fennoscandia: evidence from southwestern Norway and the northern North Sea region,
861 Quaternary Science Reviews 19, 667–685.

862 Sejrup, H.P., Larsen, E., Haflidason, H., Berstad, I.M., Hjelstuen, B.O., Jonsdottir, H., King, E.L., Landvik,
863 J.Y., Longva., O., Nygård, A., Ottesen, D., Raunholm, S., Rise, L., Stalsberg, K. 2003. Configuration,
864 history and impact of the Norwegian Channel Ice Stream. Boreas 32, 18–36.

865 Sejrup, H.P., Nygard, A., Hall, A.M., Haflidason, H. 2009. Middle and late Weichselian (Devensian)
866 glaciation history of south-western Norway, North Sea and eastern UK. Quaternary Science Reviews
867 28, 370–380.

868 Sejrup, H.P., Clark, C.D. and Hjelstuen, B.O. 2016. Rapid ice sheet retreat triggered by ice stream
869 debuttressing: Evidence from the North Sea. Geology 44, 355–358.

870 Stewart, M.A., Lonergan, L., Hampson, G.J. 2013. 3D seismic analysis of buried tunnel valleys in the
871 central North Sea: morphology, cross-cutting generations and glacial history. Quaternary Science
872 Reviews 72, 1–17.

873 Stewart, M.A., Lonergan, L. 2011. Seven glacial cycles in the middle-late Pleistocene of northwest
874 Europe; geomorphic evidence from buried tunnel valleys. Geology 39, 283–286.

875 Stoker, M.S., Balson, P.S., Long, D., Tappin, D.R. 2011. An overview of the lithostratigraphical
876 framework for the Quaternary deposits on the United Kingdom continental shelf. British Geological
877 Survey Research Report RR/11/03. 48 pp.

878 Stride, A.H. 1959. On the Origin of the Dogger Bank, in the North Sea. Geological Magazine 96, 33–44.

879 Sutherland, J.L., Davies, B.J., Lee, J.R. 2020. A litho-tectonic event stratigraphy from dynamic Late
880 Devensian ice flow of the North Sea Lobe, Tunstall, east Yorkshire, UK. Proceedings of the Geologists
881 Association 131, DOI:10.1016/j.pgeola.2020.03.001.

882 Valentin, H. 1955. Die Grenze der letzten Vereisung im Nordseeraum. Verhandl. Deut. Geografentag,
883 Hamburg 30, 359–366.

884 van der Meer, J.J.M., Laban, C. 1990. Micromorphology of some North Sea till samples, a pilot study.
885 Journal of Quaternary Science 5, 95–101.

886 Van der Veen, C.J. 2002. Calving glaciers. Progress in Physical Geography, 26(1), 96–122.

887 van Gijssel, K. 1987. A lithostratigraphic and glaciotectonic reconstruction of the Lamstedt Moraine,
888 Lower Saxony (FRG). In van der Meer, J.J.M. (Ed.): Tills and Glacitectonics, 145–156, A.A. Balkema,
889 Rotterdam.

890 Vaughan-Hirsch, D., Phillips, E. 2017. Mid-Pleistocene thin-skinned glaciotectonic thrusting of the
891 Aberdeen Ground Formation, Central Graben region, central North Sea. Journal of Quaternary Science
892 32, 196–212.

893 Veenstra, H.J. 1965. Geology of the Dogger Bank area, North Sea. Marine Geology 3, 245–262.

894 Zanella, E., Coward, M.P. 2003. Structural framework. In: Evans, D., Graham, C., Atmour, A., Bathurst,
895 P. (eds) The Millennium Atlas: Petroleum Geology of the Central and Northern North Sea. The
896 Geological Society of London, London. 45–59.

897

898 12. Figures

899 **Fig. 1.** Map showing the location of the Dogger Bank in the southern North Sea basin, and the Round
900 3 windfarm zone (study area) indicated by the red polygon. Also shown are a number of published ice
901 sheet extents during the last glaciation, highlighting the uncertainty in interpreting maximum ice
902 extents within the southern North Sea. The limit of the UK territorial waters is also marked in red.
903 EMODNET DigBath bathymetry (UK waters) and GEBCO bathymetry (non-UK waters).

904 **Fig. 2. (a)** Horizon map constructed for the top of the deformed lower part of the Dogger Bank
905 Formation which underlies the western part of Dogger Bank (see text for details). Also shown are the
906 location of the seismic profiles analysed during this present study. **(b)** Landform map of the buried
907 glacial landscape concealed within the Dogger Bank Formation comprising a suite of topographically
908 higher arcuate moraine ridges separated by lower lying sedimentary basins areas and meltwater
909 channels (after Phillips *et al*., 2018). Seismic profiles 1 to 20 refer to the geological cross sections
910 referred to in text and illustrated in Figs. 4 to 13. FTC – fold and thrust complex; TBM – thrust-block
911 moraine, LB – large sedimentary basins.

912 **Fig. 3.** Geological cross sections constructed for seismic profiles 1 to 4 from Area A (see Fig. 2): **(a)**
913 seismic profile 1; **(b)** seismic profile 2; **(c)** seismic profile 3; and **(d)** seismic profile 4. A high-resolution,
914 large format version of this figure is available as a supplementary publication or from the lead author
915 on request.

916 **Fig. 4a.** Geological cross sections constructed for seismic profiles 5 to 8 from Area B (see Fig. 2): **(a)**
917 seismic profile 5; **(b)** seismic profile 6; **(c)** seismic profile 7; and **(d)** seismic profile 8. A high-resolution,
918 large format version of this figure is available as a supplementary publication or from the lead author
919 on request.

920 **Fig. 4b.** Geological cross sections constructed for seismic profiles 9 to 12 from Area B (see Fig. 2): **(e)**
921 seismic profile 9; **(f)** seismic profile 10; **(g)** seismic profile 11; and **(h)** seismic profile 12. A high-
922 resolution, large format version of this figure is available as a supplementary publication or from the
923 lead author on request.

Fig. 4c. Geological cross sections constructed for seismic profiles 13 to 15 from Area B (see Fig. 2): **(i)** seismic profile 13; **(j)** seismic profile 14; and **(k)** seismic profile 15. A high-resolution, large format version of this figure is available as a supplementary publication or from the lead author on request.

Fig. 5. Geological cross sections constructed for seismic profiles 16 to 20 from Area C (see Fig. 2): **(a)** seismic profile 16; **(b)** seismic profile 17; **(c)** seismic profile 18; **(d)** seismic profile 19; and **(e)** seismic profile 20. A high-resolution, large format version of this figure is available as a supplementary publication or from the lead author on request.

Fig. 6. Geological cross section and interpreted seismic data for the central part of seismic profile 11 (see text for details). TBM – thrust-block moraine.

Fig. 7. Geological cross section and interpreted seismic data for the northeastern part of seismic profile 10 (see text for details). TBM – thrust-block moraine.

Fig. 8. Geological cross section and interpreted seismic data for the southwestern part of seismic profile 11 (see text for details). FTC – thrust and fold complex; TBM – thrust-block moraine.

Fig. 9. Geological cross section and interpreted seismic data for the southwestern part of seismic profile 7 (see text for details).

Fig. 10. Geological cross section and interpreted seismic data for the southwestern part of seismic profile 10 (see text for details). FTC – thrust and fold complex.

Fig. 11. Geological cross section and interpreted seismic data for the central and northern parts of seismic profile 9 (see text for details). FTC – thrust and fold complex; TBM – thrust-block moraine.

Fig. 12. Geological cross section and interpreted seismic data for the southwestern part of seismic profile 5 (see text for details). FTC – thrust and fold complex; TBM – thrust-block moraine.

Fig. 13. Cartoon showing the proposed configuration of the North Sea and Dogger Bank lobes on Dogger Bank when they reached their maximum extent during the last glaciation.

Fig. 14. Diagram showing the proposed glacitectonic and sedimentary evolution of the western Dogger Bank area.

13. Tables

Table 1. Summary of the characteristics of the basal, lower and upper Dogger Bank identified on the seismic profiles (Phillips *et al.*, 2018).

Seismic subunit	Description
Basal Dogger Bank (BDB)	Structurally lowest unit within the Dogger Bank Formation (0-30 m thick); distinguished by its overall brighter appearance on the seismic profiles; upper surface marked by a band of bright reflectors interpreted as a prominent desiccation/weathering surface; varies from acoustically "massive"/"structureless" to containing laterally variably dipping reflectors; reflectors locally appear crenulated/folded and/or disrupted due to glacitectonic deformation; base interpreted as a laterally extensive décollement surface
Lower Dogger Bank (LDB)	Represents main deformed part of Dogger Bank Formation (up to 40-50 m thick); acoustic appearance highly variable ranging from acoustically "blank", lacking internal reflectors and apparently internally "massive"/"structureless", through to stratified, containing weakly to strongly developed reflectors; laterally variably dipping reflectors; reflectors locally appear folded and/or disrupted due to glacitectonic deformation; upper surface locally marked by a band of bright reflectors interpreted as a desiccation/weathering surface
Upper Dogger Bank (UDB)	Structurally highest unit within the Dogger Bank Formation (0-50 m thick); acoustic character is laterally variable ranging from areas with no ("blank") or very weakly developed reflectors through to sections with moderately to strongly developed subhorizontal (bedding) to inclined (foresets) reflectors; base of unit irregular (erosive) and clearly truncates structures identified within the underlying subunits

953

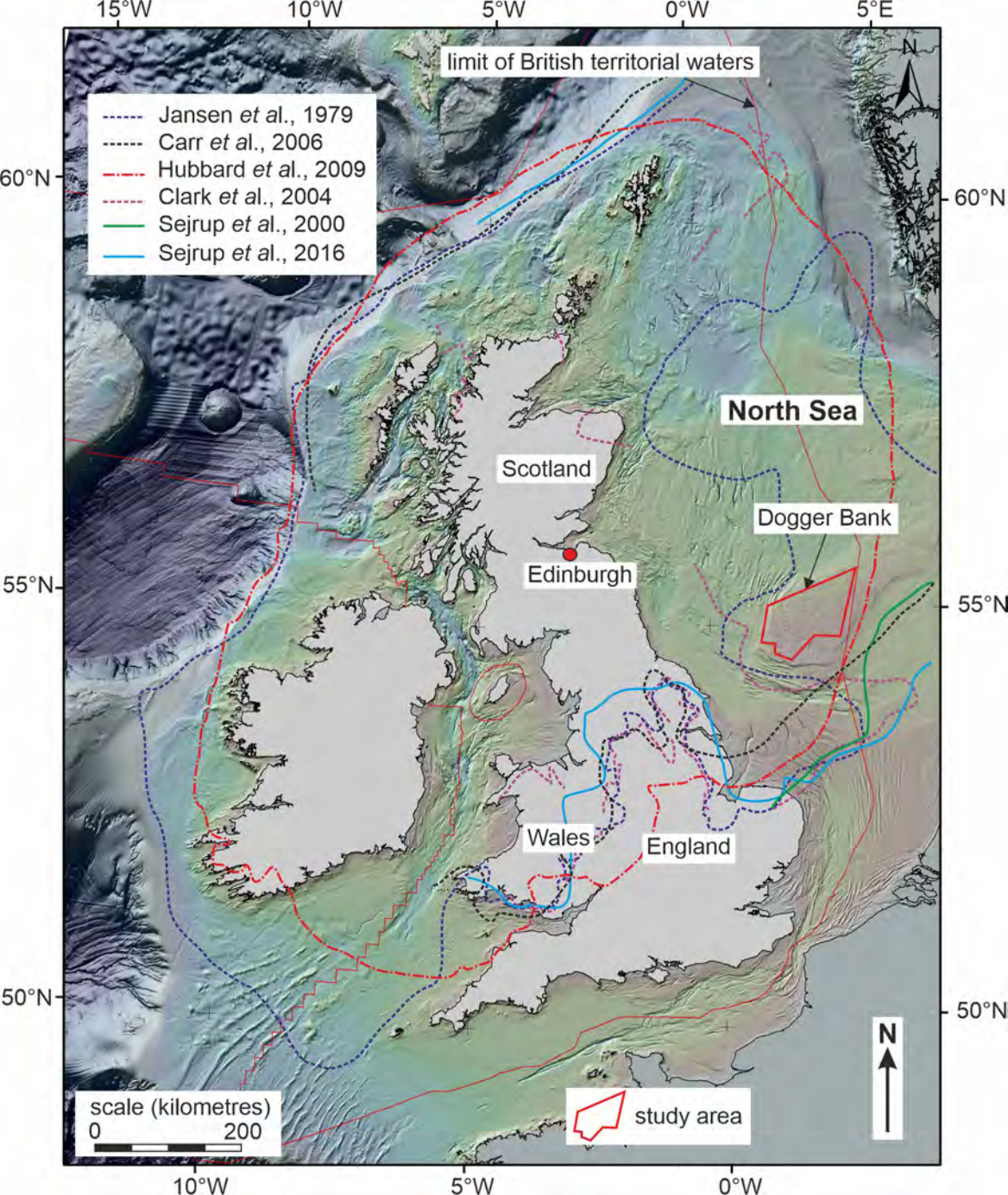
15°W
10°W
5°W
0°W
5°E
60°N
55°N
50°N
limit of British territorial waters
Jansen et al., 1979
Carr et al., 2006
Hubbard et al., 2009
Clark et al., 2004
Sejrup et al., 2000
Sejrup et al., 2016
North Sea
Scotland
Edinburgh
Dogger Bank
Wales
England
N
scale (kilometres)
0
200
study area

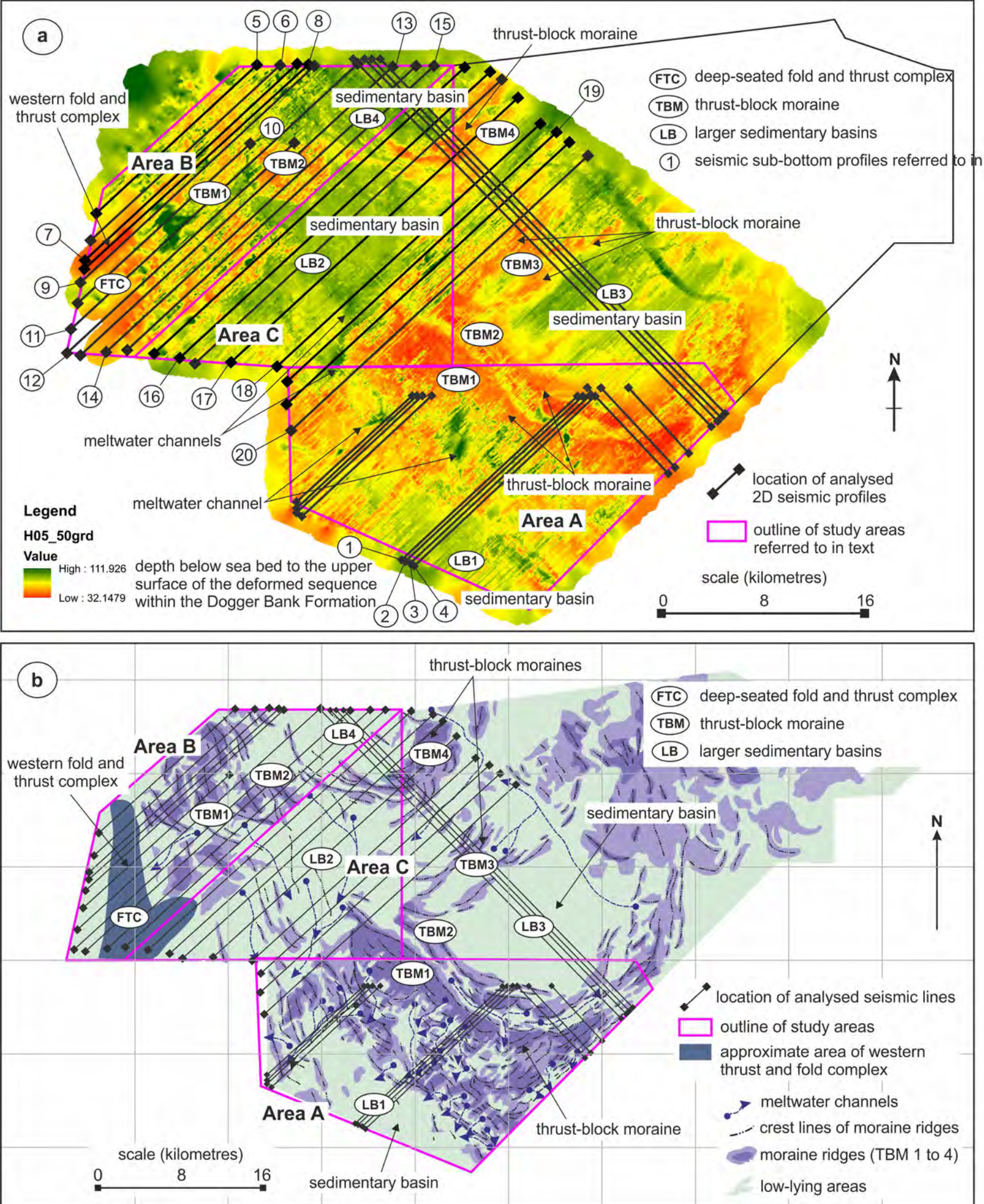
a
thrust-block moraine
western fold and thrust complex
sedimentary basin
Area B
Area C
Area A
meltwater channels
meltwater channel
thrust-block moraine
sedimentary basin
thrust-block moraine
sedimentary basin
sedimentary basin
FTC deep-seated fold and thrust complex
TBM thrust-block moraine
LB larger sedimentary basins
1 seismic sub-bottom profiles referred to in text
N
location of analysed 2D seismic profiles
outline of study areas referred to in text
scale (kilometres)
0 8 16
Legend
H05_50grd
Value
High : 111.926
Low : 32.1479
depth below sea bed to the upper surface of the deformed sequence within the Dogger Bank Formation
b
thrust-block moraines
western fold and thrust complex
Area B
Area C
Area A
sedimentary basin
thrust-block moraine
sedimentary basin
FTC deep-seated fold and thrust complex
TBM thrust-block moraine
LB larger sedimentary basins
N
location of analysed seismic lines
outline of study areas
approximate area of western thrust and fold complex
meltwater channels
crest lines of moraine ridges
moraine ridges (TBM 1 to 4)
low-lying areas
scale (kilometres)
0 8 16

Area A: cross-sections through the shallow subsurface of Dogger Bank (after Phillips *et al.*, 2018)

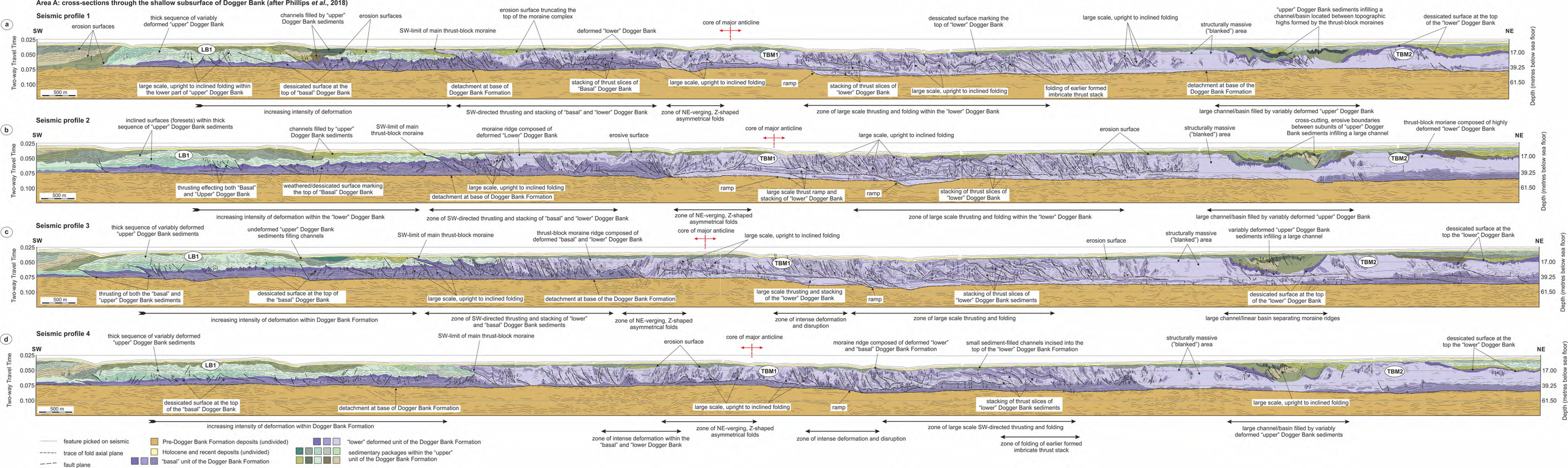

Area B: cross-sections through the shallow subsurface of Dogger Bank

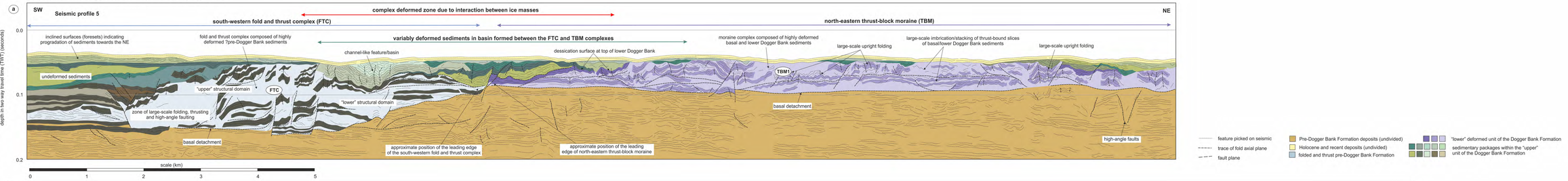

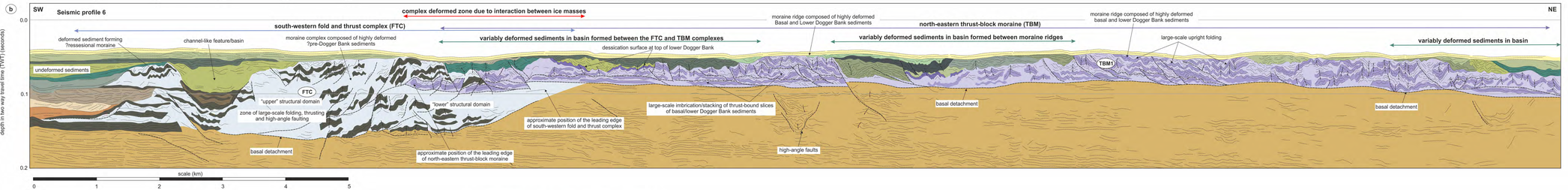

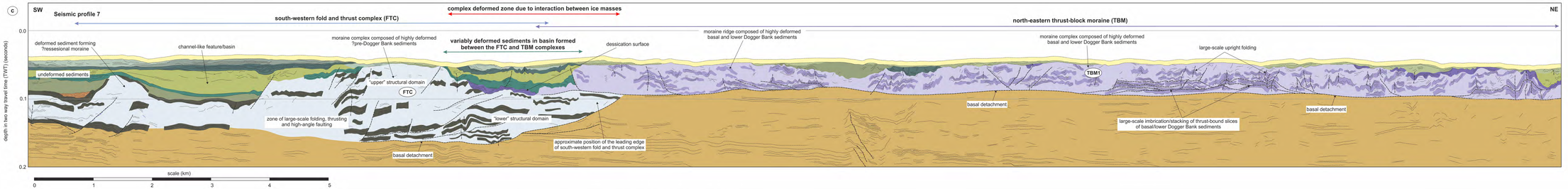

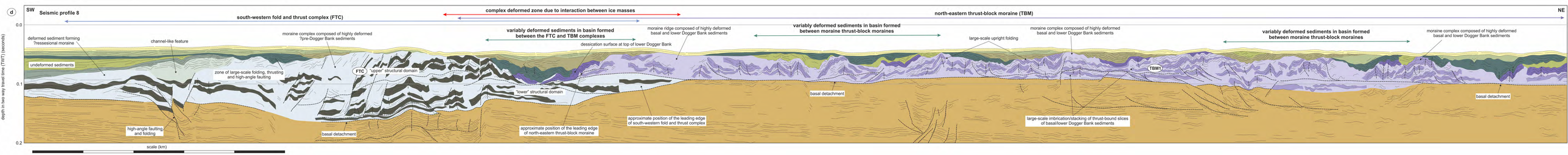

Area B: cross-sections through the shallow subsurface of Dogger Bank

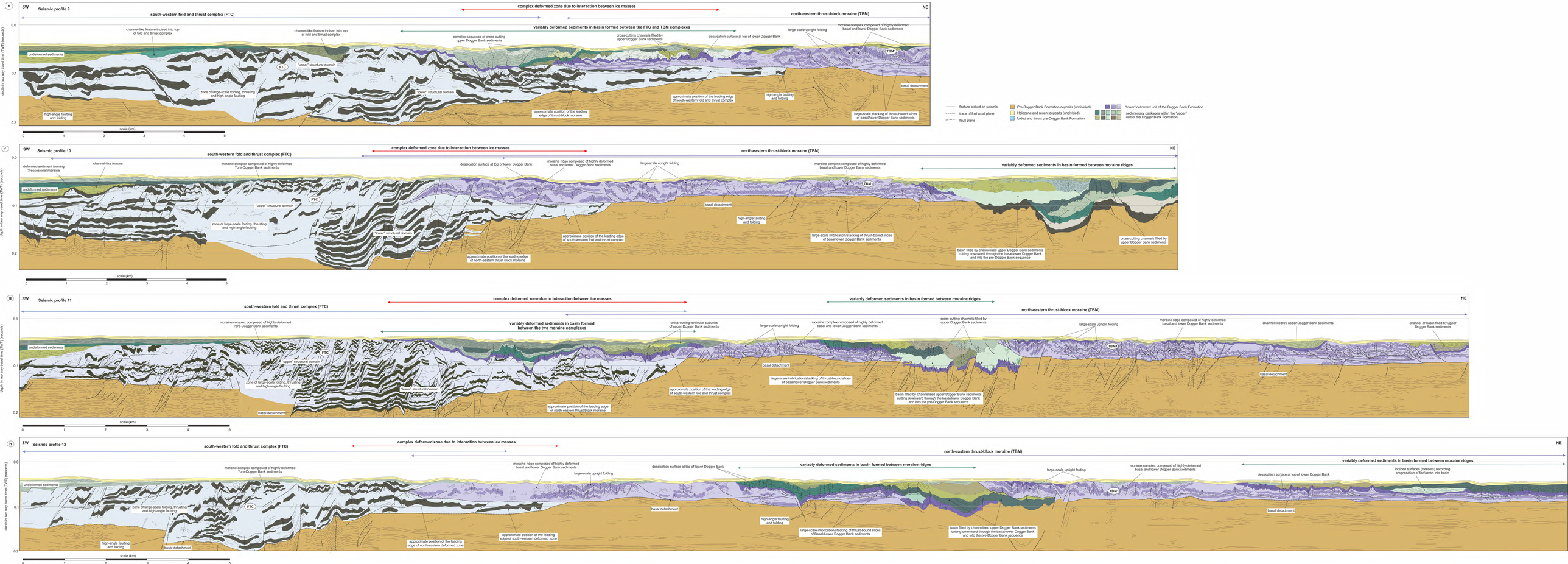

Area B: cross-sections through the shallow subsurface of Dogger Bank

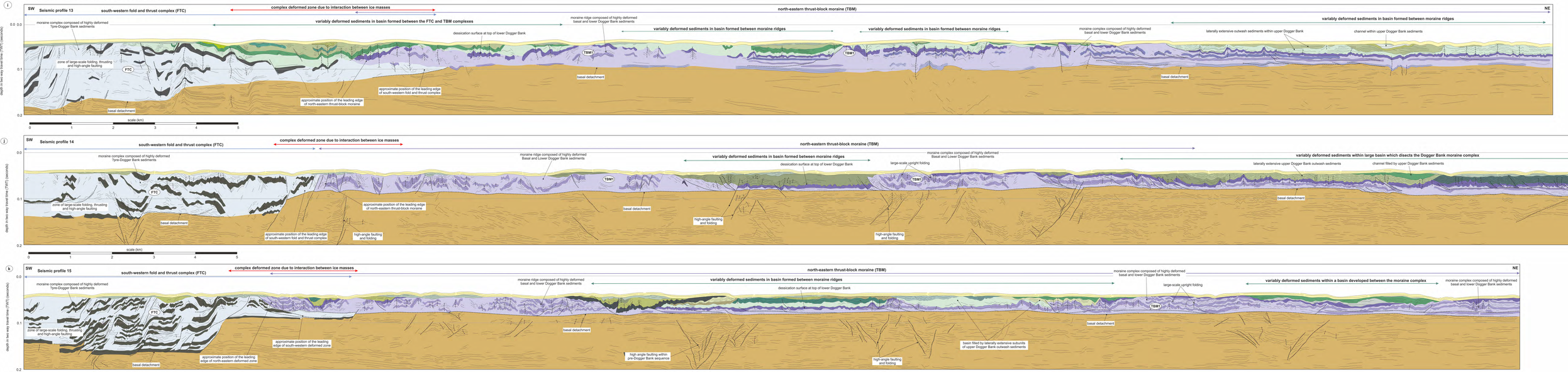

Area C: cross-sections through the shallow subsurface of Dogger Bank

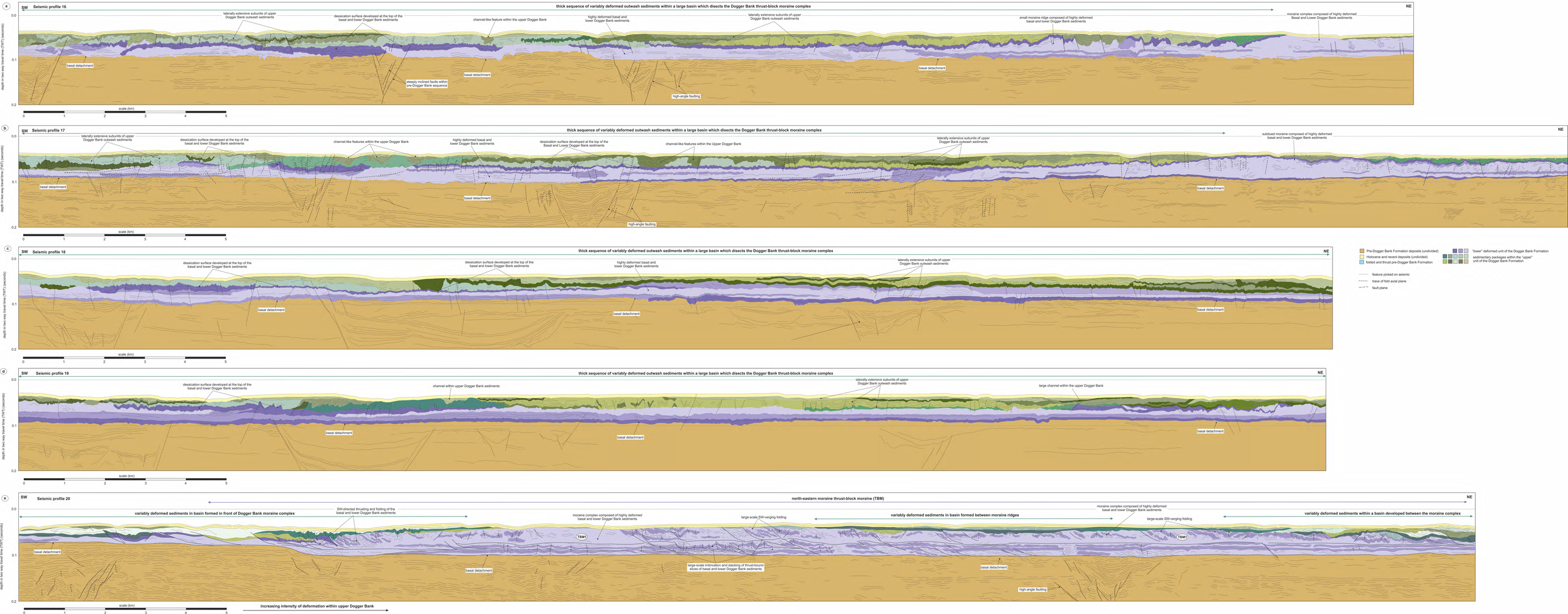

Central part of seismic profile 11

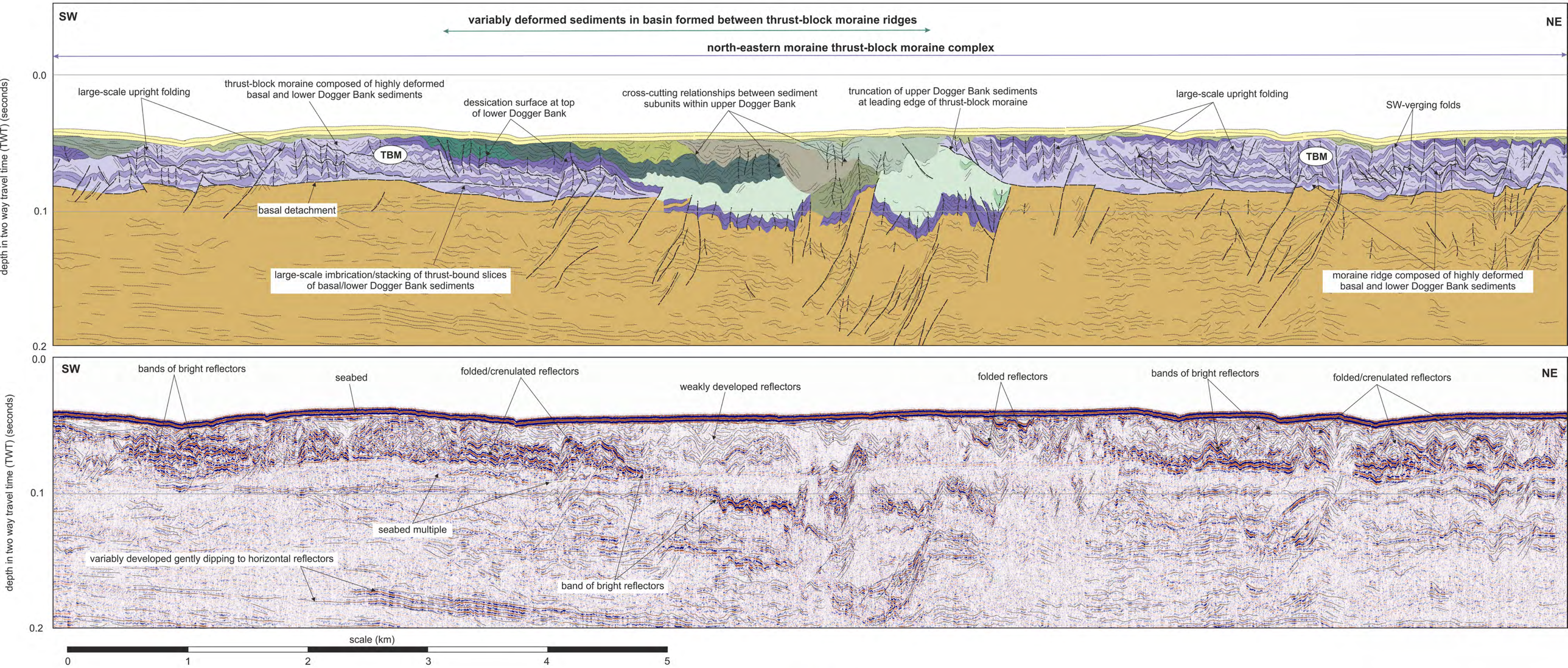

Northeastern part of seismic profile 10

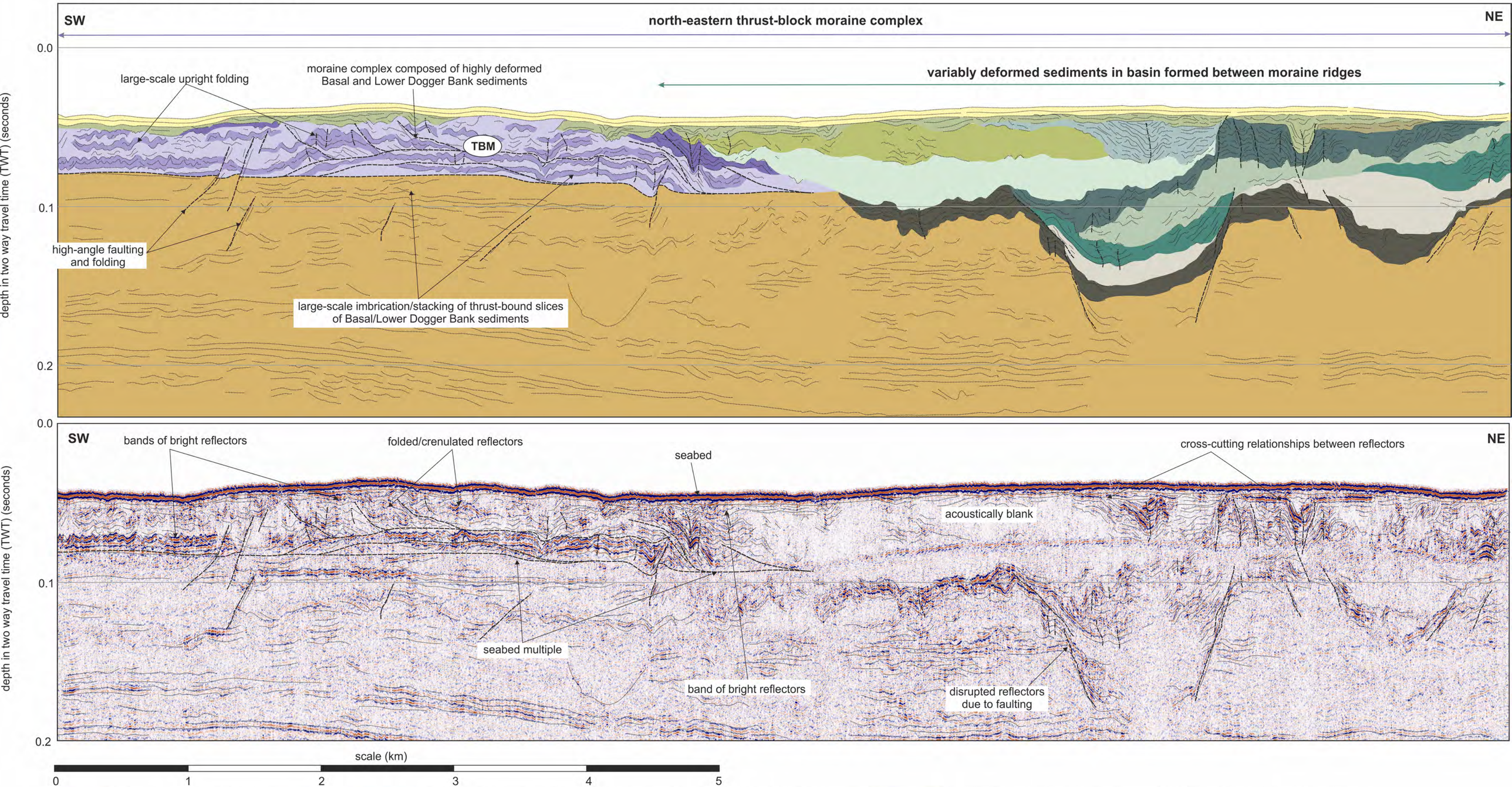

Southwestern part of seismic profile 11

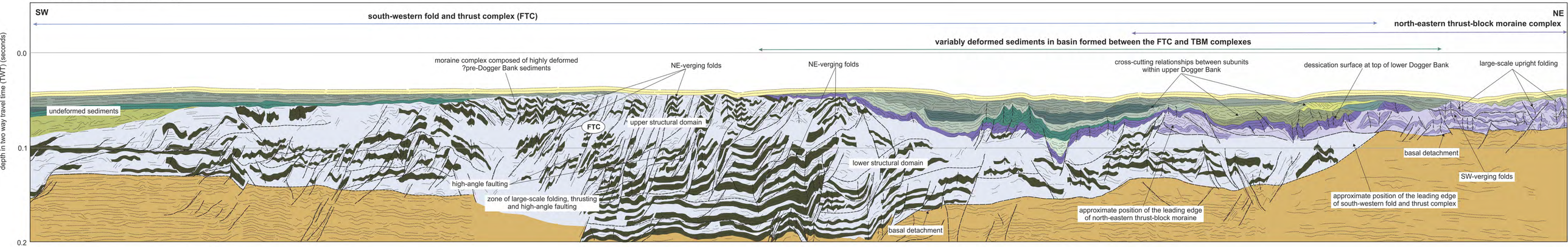

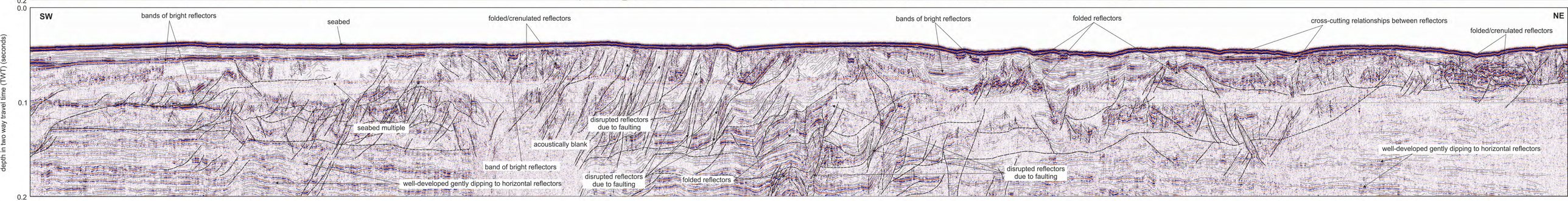

scale (km)

0 1 2 3 4 5

post-glacial Holocene sediments

pre-Dogger Bank Formation sequence undivided

undeformed to weakly deformed sediments including upper Dogger Bank sequence

reflectors picked on seismic adata

highly deformed sediments including basal and lower Dogger Bank sequences

faults and thrusts

fold axes

highly deformed sediments of the south-western fold and thrust complex

Southwestern end of Seismic Profile 7

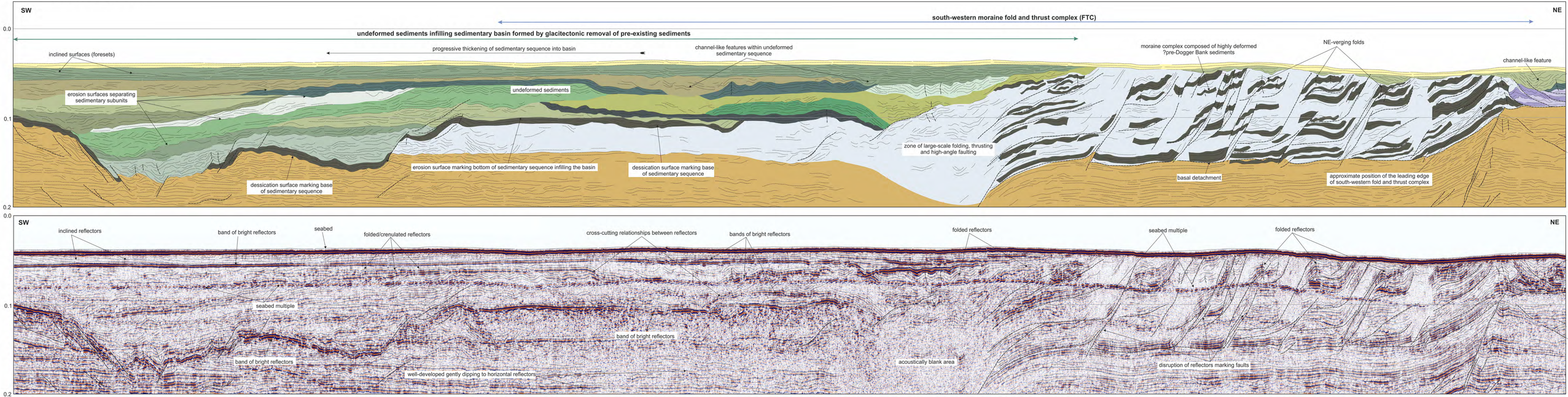

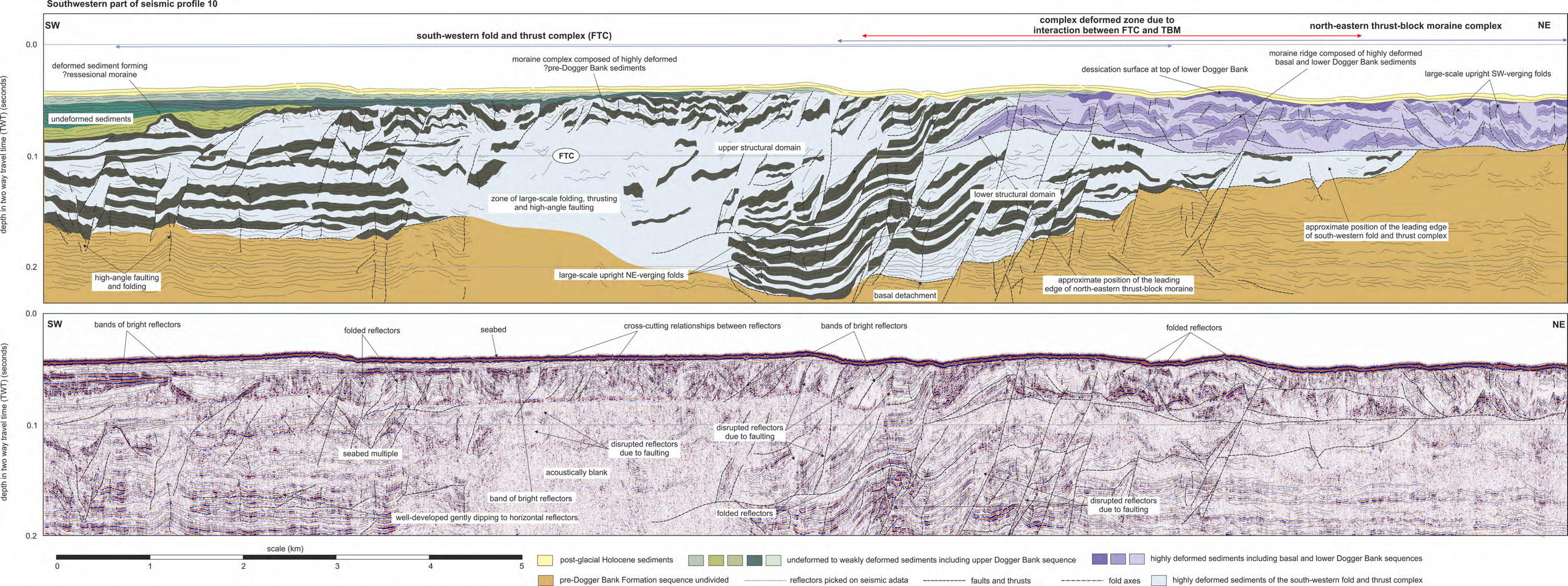
Southwestern part of seismic profile 10
SW
NE
south-western fold and thrust complex (FTC)
complex deformed zone due to interaction between FTC and TBM
north-eastern thrust-block moraine complex
depth in two way travel time (TWT) (seconds)
0.0
0.1
0.2
deformed sediment forming ?ressesional moraine
moraine complex composed of highly deformed ?pre-Dogger Bank sediments
dessication surface at top of lower Dogger Bank
moraine ridge composed of highly deformed basal and lower Dogger Bank sediments
large-scale upright SW-verging folds
undeformed sediments
FTC
upper structural domain
zone of large-scale folding, thrusting and high-angle faulting
lower structural domain
approximate position of the leading edge of south-western fold and thrust complex
high-angle faulting and folding
large-scale upright NE-verging folds
basal detachment
approximate position of the leading edge of north-eastern thrust-block moraine
bands of bright reflectors
folded reflectors
seabed
cross-cutting relationships between reflectors
bands of bright reflectors
folded reflectors
disrupted reflectors due to faulting
seabed multiple
disrupted reflectors due to faulting
acoustically blank
band of bright reflectors
folded reflectors
disrupted reflectors due to faulting
well-developed gently dipping to horizontal reflectors
scale (km)
0
1
2
3
4
5
post-glacial Holocene sediments
undeformed to weakly deformed sediments including upper Dogger Bank sequence
highly deformed sediments including basal and lower Dogger Bank sequences
pre-Dogger Bank Formation sequence undivided
reflectors picked on seismic adata
faults and thrusts
fold axes
highly deformed sediments of the south-western fold and thrust complex

Central and northern part of seismic profile 9

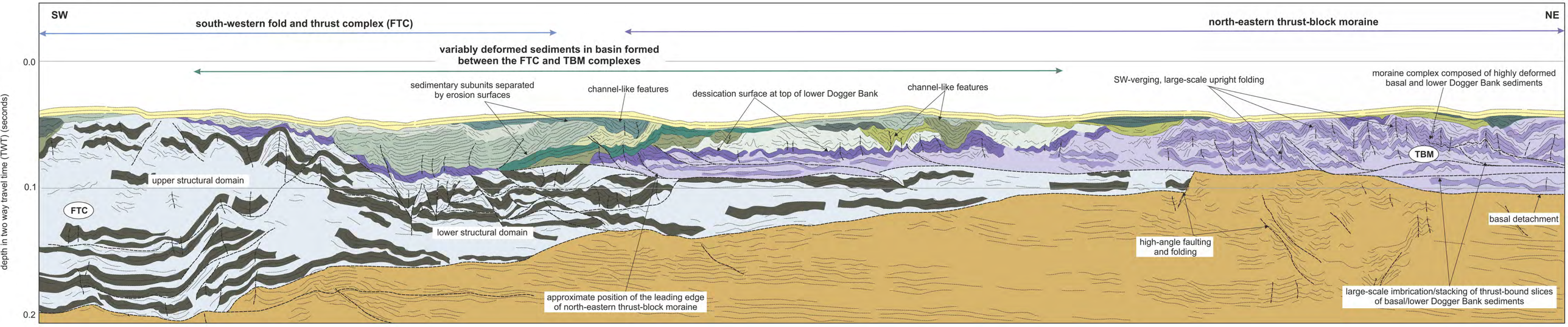

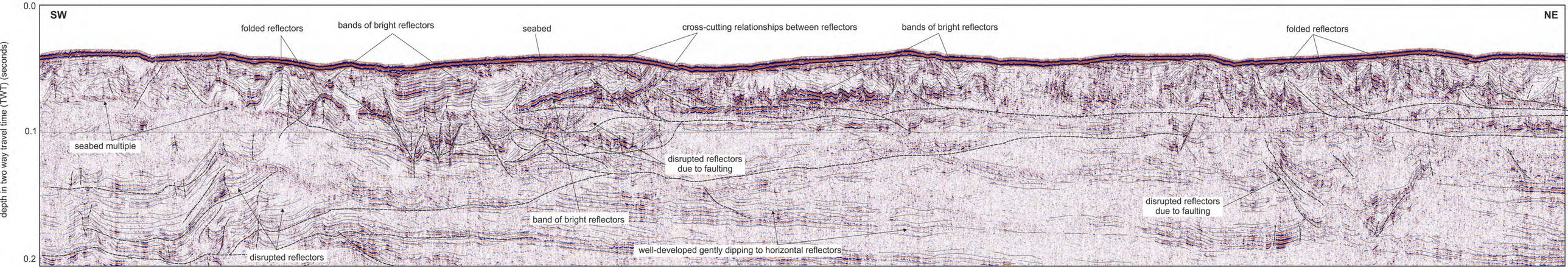

scale (km)

0 1 2 3 4 5

post-glacial Holocene sediments

undeformed to weakly deformed sediments including upper Dogger Bank sequence

highly deformed sediments including basal and lower Dogger Bank sequences

pre-Dogger Bank sequence undivided

reflectors picked on seismic profiles

faults and thrusts

fold axes

highly deformed sediments of the south-western fold and thrust complex

Southwestern part of seismic profile 5

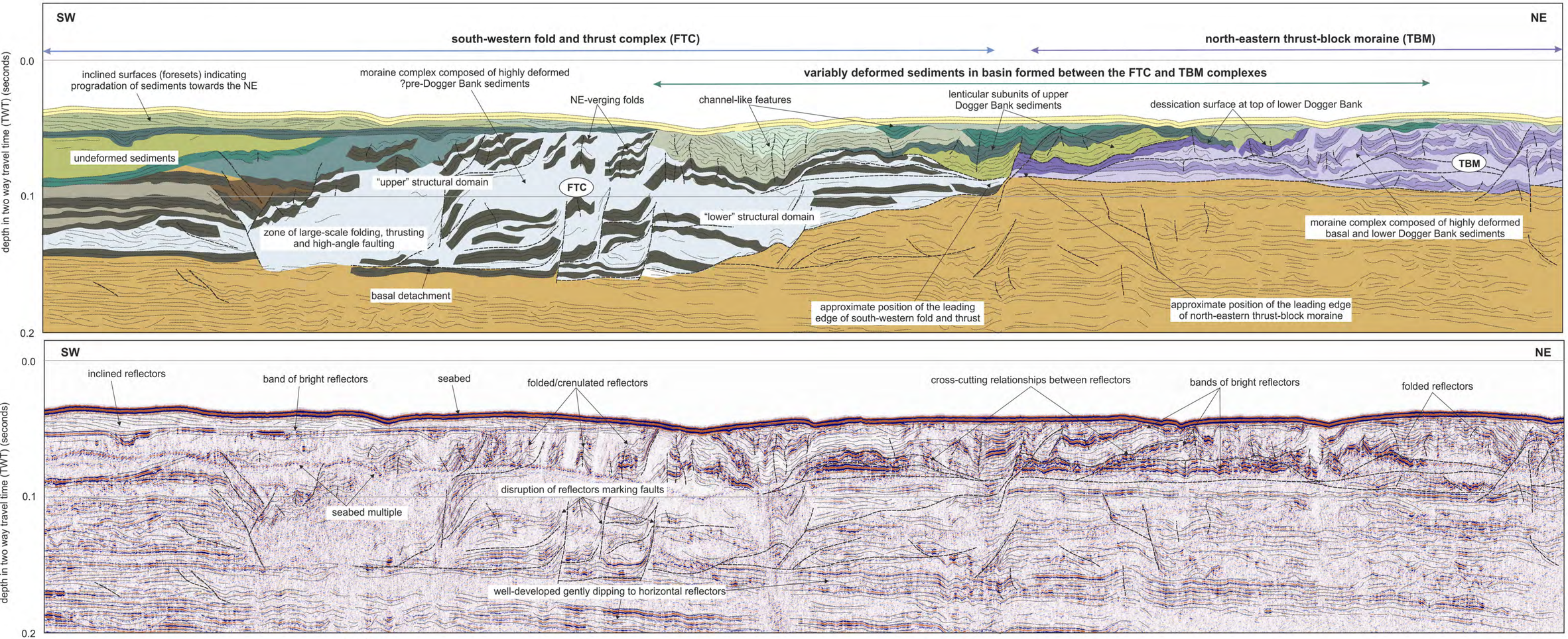

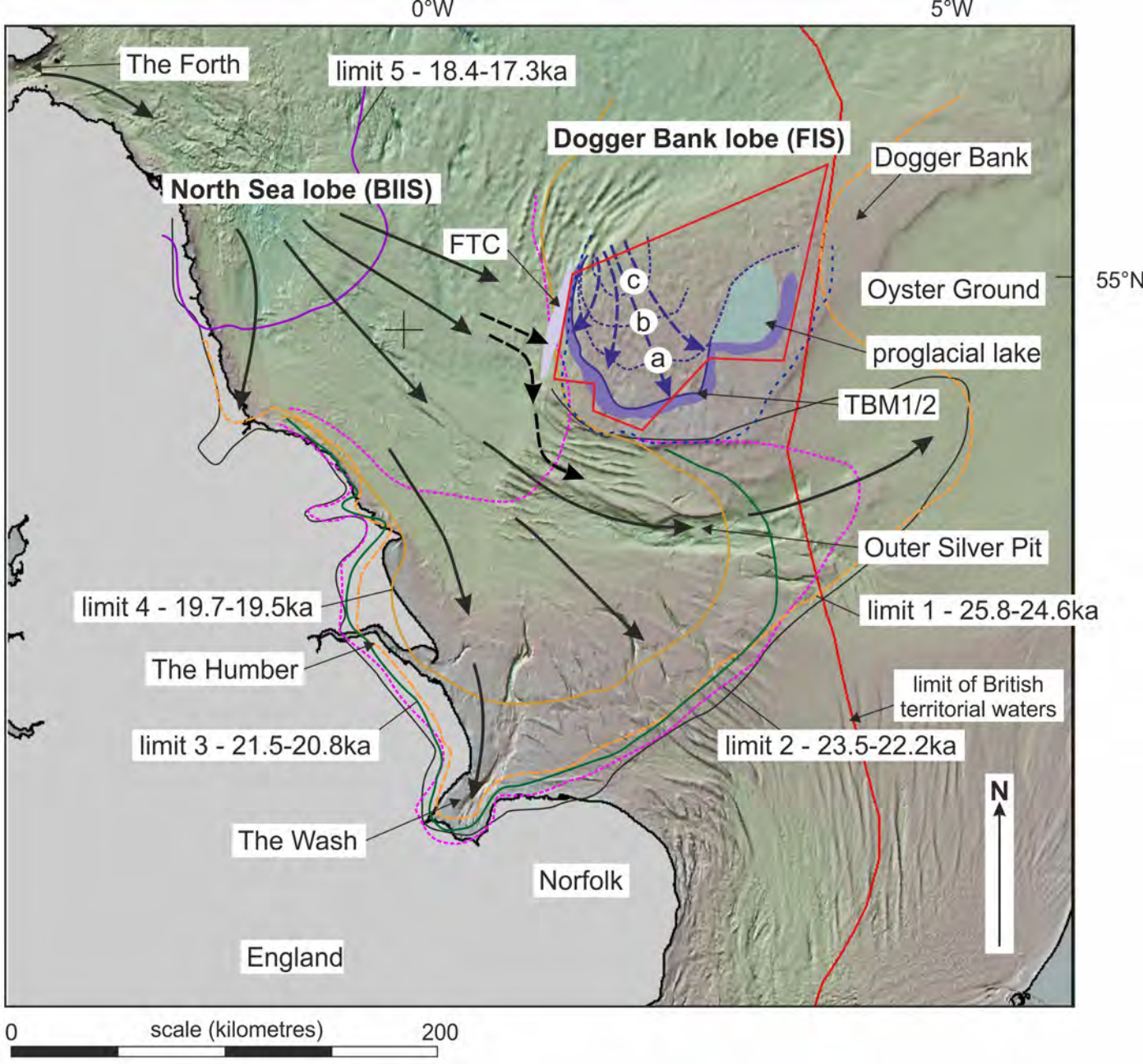

windfarm area

a to c - approximate positions of the actively retreating Dogger Bank lobe

possible maximum limit of the Dogger Bank lobe

limit of the Bolders Bank Formation

dominant ice movement direction of the Dogger Bank lobe (FIS)

dominant ice movement direction of the North Sea lobe (BIIS)

ice movement direction associated with the formation of the fold and thrust complex on the western margin of Dogger Bank

ice sheet limits 1 to 5 and associated ages taken from Evans *et al.*, (2021)

a

Area B
LB4
TBM2
TBM4
TBM1
readvance phase C thrust-block moraines
readvance phase B thrust-block moraines
TBM3
FTC
LB2
LB3
Area C
TBM2
TBM1
readvance phase A thrust-block moraines
Area A
LB1
N
Legend
H05_50grd
Value
High : 111.926
Low : 32.1479
depth below sea bed to the upper surface of the deformed sequence within the Dogger Bank Formation
0
scale (kilometres)
16

b

development of a marginal basin between the two ice masses
Initial stages of retreat of the Dogger Bank ice
Dogger Bank ice
FTC
development of the deep-seated fold and thrust complex
British and Irish Ice Sheet
LB1
N
0
scale (kilometres)
16

c

Readvace phase A: active retreat of the Dogger Bank ice
meltwater draing southwards between retreating ice sheets
TBM1
Dogger Bank ice
increasing complexity of thrust-block moraines formed at margin of actively retreating ice sheet
LB2
FTC
TBM1
possible retreat of ice sheet from western edge of Dogger Bank and deposition of outwash
LB1
outwash deposited infront of retreating ice sheet margin
N
0
scale (kilometres)
16

d

Readvance phase B of the Dogger Bank ice during active retreat
TBM2
TBM1
Dogger Bank ice
continued retreat leading to the formation of sedimentary basins between the thrust-block moraines
LB2
TBM3
LB3
FTC
TBM2
TBM1
meltwater draining through “breach” between thrust-block morianes
LB1
N
0
scale (kilometres)
16

e

Readvance phase C during the later stages of retreat of the Dogger Bank ice
progressive filling of sedimentary basin by outwash
LB4
TBM2
TBM4
TBM1
TBM3
FTC
LB2
LB3
meltwater draining through “breach” between thrust-block moraines
TBM2
TBM1
retreat of ice sheet from western edge of Dogger Bank and deposition of outwash
LB1
N
0
scale (kilometres)
16

ice movement direction
meltwater channels
crestlines of thrust block moraines
FTC deep-seated fold and thrust complex
TBM thrust-block moraine
LB larger sedimentary basins